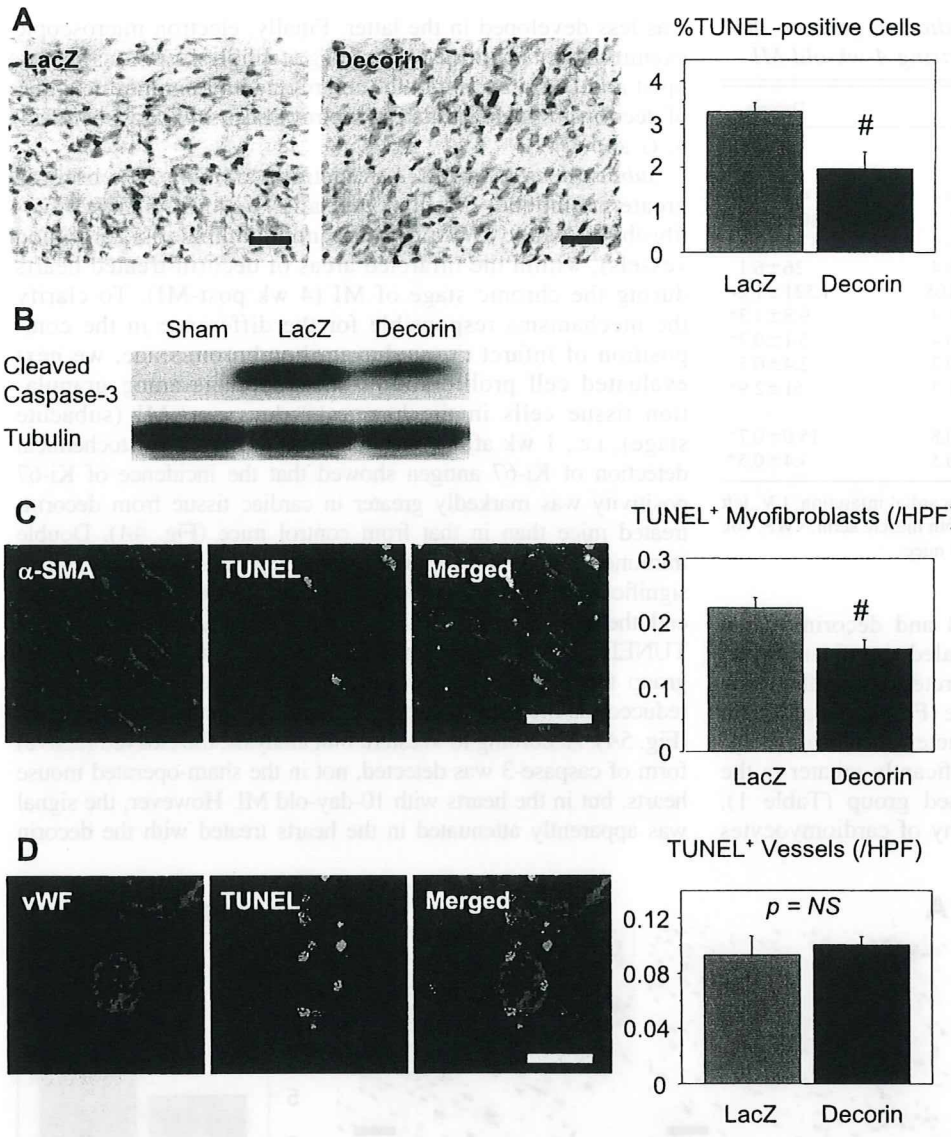

Fig. 5. Apoptosis within granulation tissue 10 days post-MI. *A*: photomicrographs showing terminal deoxynucleotidyl transferase-mediated in situ nick-end labeling (TUNEL)-positive cells (*left*) with a graph comparing the incidences of TUNEL positivity in each group (*right*). *B*: Western blot for the cleaved (activated) caspase-3. *C* and *D*, *left*: confocal photomicrographs of tissue sections from a LacZ-treated heart subjected to TUNEL (green fluorescence) and immunolabeled with antibody against α-SMA (*C*) or vWF (*D*) (red fluorescence). Scale bars, 20 μm. *Right*: graphs showing the incidences of TUNEL positivity separately evaluated in myofibroblasts and endothelial cells. Bars in graphs are means ± SE. #$P <$ 0.05 vs. LacZ-treated MI mice.

gene (Fig. 5*B*). Further analysis using double immunofluorescent labeling revealed that decorin treatment significantly reduced the incidence of TUNEL positivity among myofibroblasts, but not endothelial cells (Fig. 5, *C* and *D*). Next, we investigated necrosis by immunohistochemistry for C9, which is a part of the membrane attacking complex C5b-9 (11). No C9-immunopositive necrotic cell was found in granulation tissue cells of any groups (photographs not shown). This finding is consistent with previous electron microscopic studies showing that the dying mode of postinfarct granulation tissue cells is not necrosis, but apoptosis (9, 37, 51).

To check whether the treatment promoted viable cardiomyocytes to replace the function of the infarcted area, we examined cell proliferation activity and apoptosis in the salvaged myocardium. Double immunofluorescence for myoglobin and Ki-67 revealed no proliferating cardiomyocyte in viable myocardium 10 days post-MI (Fig. 6*A*). We noted TUNEL-positive nuclei of cardiomyocytes in viable myocardium. However, they were extremely rare in each group, and there was no significant difference in the prevalence between the groups (10 days post-MI: sham operated group, 0.012 ± 0.007%; LacZ-treated MI group, 0.010 ± 0.008%; decorin-treated MI group, 0.013 ± 0.011%). These findings do not support the possibility that the present treatments increased regeneration or reduced cell loss due to apoptosis of viable cardiomyocytes to replace the infarcted area.

Western blot analysis showed that expression of TGF-β was significantly upregulated in heart tissues collected on *day 10* post-MI (Fig. 7). Moreover, we observed marked activation (phosphorylation) of Smad2 and Smad3, two downstream mediators of TGF-β. Although decorin treatment did not affect TGF-β or endogenous (mouse) decorin expression, it significantly suppressed Smad2 and Smad3 activation (Fig. 7), which implies that inhibition of signaling in the TGF-β/Smad2/Smad3 pathway contributes substantially to the beneficial effects exerted by decorin against post-MI cardiac remodeling and heart failure. PAI-1 is one of the other important team players in fibrosis (56). Myocardial PAI-1 expression was unchanged in the heart 10 days post-MI, which was not influenced by the decorin gene therapy either (Fig. 7).

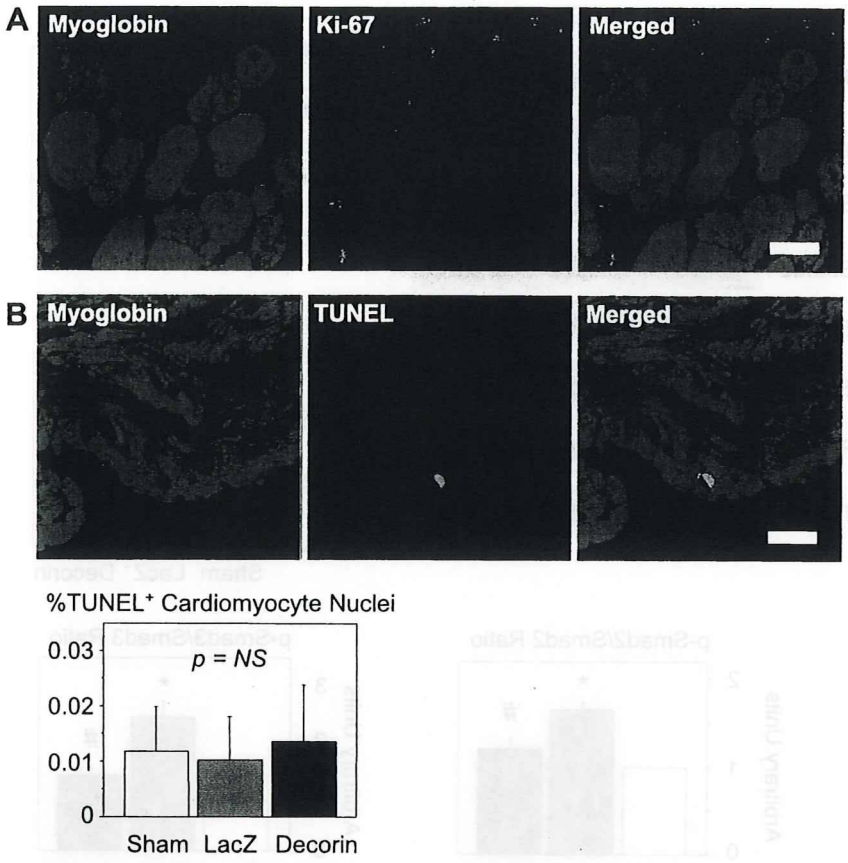

Fig. 6. Cell proliferation and TUNEL positivity of the salvaged cardiomyocytes 10 days post-MI. *A*: confocal photomicrographs of tissue sections from a decorin-treated heart subjected to double immunofluorescence for Ki-67 (green fluorescence) and myoglobin (red fluorescence). There was no Ki-67-positive cardiomyocyte on the preparation where some Ki-67-positive granulation tissue cells or interstitial cells were noted. *B*: confocal photomicrographs of tissue sections from a LacZ-treated heart subjected to double immunofluorescence for TUNEL (green fluorescence) and myoglobin (red fluorescence). TUNEL-positive nuclei of cardiomyocytes were noted, although very rarely. Graph shows the incidences of TUNEL-positive nuclei in cardiomyocytes. Scale bars, 20 μm. Values in graphs are means ± SE.

DISCUSSION

Our findings provide the first evidence that postinfarction decorin gene therapy, started on *day 3* post-MI, mitigates the adverse effects on LV geometry and function during the chronic stage.

Pathophysiological mechanisms for the beneficial effects of decorin gene therapy on postinfarction heart failure. One remarkable finding of the present study is that decorin alters the geometry of the infarct scar without affecting its absolute area, i.e., the infarcted segment was thicker and had a smaller circumferential length in decorin-treated hearts during the chronic stage than in control hearts. This is noteworthy because wall stress is directly proportional to cavity diameter and inversely proportional to wall thickness (Laplace's law) (55) and because wall stress and LV remodeling (dilatation) have a vicious relationship and exacerbate one another. It is thus conceivable that the observed change in infarct geometry would greatly improve the hemodynamic state of the heart.

Our findings also suggest that infarct scar tissue is qualitatively altered by treatment with decorin gene. We observed greater numbers of cells, including abundant myofibroblasts and vascular cells, within the infarct scar in decorin-treated hearts. These cells are normally destined to disappear via apoptosis during the natural course of healing after MI (9, 51), but we found that apoptosis was significantly inhibited in decorin-treated hearts during the subacute stage (10 days post-MI). Moreover, decorin gene therapy also significantly increased cardiac proliferation of both myofibroblasts and vascular endothelial cells. These findings have two important implications. First, both diminished apoptosis and enhanced proliferation among granulation tissue cells during the subacute stage appear to contribute to the observed increase in the cell population within the scar tissue during the chronic stage, which likely preserves the infarct wall thickness. Second, myofibroblasts, which are known to play an important role in wound contraction during the healing process (12), could mediate contraction-induced reduction in the length of the infarct segment, thereby increasing infarct wall thickness. That, in turn, would alter the infarct tissue geometry, reducing wall stress and mitigating LV dilatation and dysfunction.

Vascular endothelial cells also proliferated during the granulation tissue phase in hearts treated with decorin, suggesting an angiogenic effect of decorin. Decorin suppresses malignant tumor cell-mediated angiogenesis (15), whereas it promotes angiogenesis in normal tissue during the healing stage or when ectopically expressed (45, 46). Our finding was well consistent with the latter reports on the role of decorin in angiogenesis. The function of proliferated vascular endothelial cells during the chronic stage of MI remains unclear, although it has been shown that, by supplying blood, newly formed vessels help sustain the cellular components within the infarct area (50). Recently, we reported that blood flow into the infarct area by late reperfusion promotes proliferation and inhibits apoptosis among granulation tissue cells (35). On the other hand, leukocytes continued to die. We suggest that leukocytes may have a higher sensitivity to apoptotic stimuli than other preserved cells, because inflammatory cells generally show very active

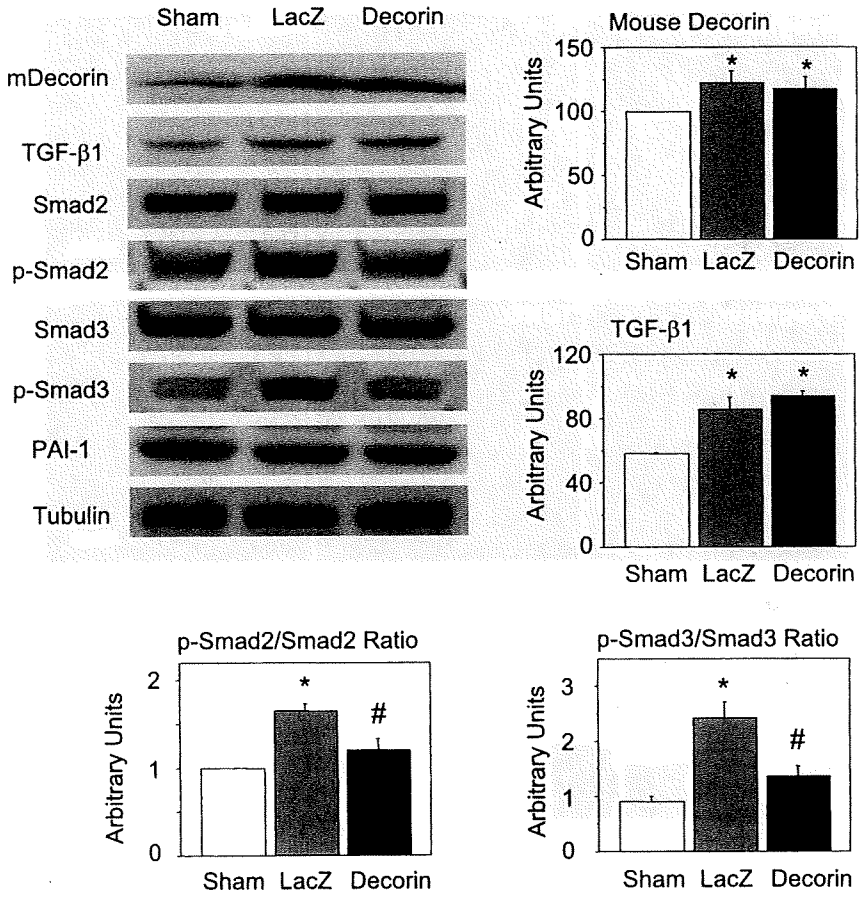

Fig. 7. Western blot analysis for endogeous mouse decorin, transforming growth factor (TGF)-β1, Smad2, Smad3, the phosphorylated (activated) forms of Smad2 (p-Smad2) and Smad3 (p-Smad3), and plasminogen activator inhibitor type 1 (PAI-1) in hearts 10 days post-MI. Graphs show the morphometric data. Values are means ± SE. $*P < 0.05$ vs. sham-operated mice; $\#P < 0.05$ vs. LacZ-treated MI mice.

proapoptotic interactions through death ligands and receptors (34).

We also observed that decorin gene therapy significantly reduces cardiac fibrosis, confirming the previously reported antifibrotic effect of decorin in hearts (21). Because myocardial fibrosis contributes to both systolic and diastolic dysfunction (5, 22), its reduction is likely another important way in which decorin may mitigate LV remodeling and heart failure.

In contrast to granulation tissue cells, TUNEL positivity in salvaged cardiomyocytes was not affected by the decorin gene therapy, suggesting no contribution of cardiomyocyte death via apoptosis to the beneficial effects of the therapy. The prevalence of TUNEL-positive cardiomyocyte nuclei was very rare (~0.01%). Although the value is consistent with the previous reports, including ours (38, 44), the discrepancy of the values reported is surprisingly great, ranging from 0.02 to 12% among the studies using mouse model of subacute to chronic stage MI: maximally 600-fold difference (38, 44, 49). It may be problematic that such a critical discrepancy in the TUNEL-positive cardiomyocyte rates remains not yet reconciled, the reason of which should be elucidated in the future.

Ki-67-positive nuclei were not immunohistochemically detected in cardiomyocytes under the present staining conditions. However, immunohistochemical negativity does not always deny the slight expression of an antigen, because the sensitivity depends on the staining conditions. On the other hand, too much sensitivity may violate specificity. Beltrami et al. (2) previously reported cardiomyocyte proliferation by immunohistochemistry in human hearts with MI. It is possible that our immunostaining method for Ki-67 is relatively less sensitive compared with that of the previous report. Notwithstanding, we did detect Ki-67 expression in the granulation tissue cells on the same immunohistochemical preparations, suggesting that our immunohistochemistry was not too insensitive. Difference in immunohistochemical sensitivity and difference in species might have yielded the discrepancy between the studies. The infarct wall did not show a significant systolic thickening, even in the decorin-treated groups, unlikely supporting a possible increase of cardiomyocyte population through increased regeneration and/or reduced apoptosis by the treatment.

Molecular mechanisms involved in the beneficial effects of decorin gene therapy. TGF-β signaling controls a diverse set of cellular processes, including cell apoptosis, differentiation, and proliferation (19, 23, 48). It has also been suggested that TGF-β signaling has both proapoptotic and profibrotic effects on the heart (29, 37). SMAD proteins are important downstream mediators of TGF-β signaling (8, 18), and their absence reportedly impairs local inflammatory responses and accelerates wound healing (1). The most recent findings indicate that loss of Smad3 (in Smad3-null mice) significantly increases myofibroblast density in healing infarcts and prevents myocardial fibrosis (4). In the present study, we observed that cardiac expression of TGF-β, p-Smad2, and p-Smad3 was strongly upregulated in control mice during the granulation tissue phase, 10 days post-MI. Notably, mice receiving the decorin gene expressed high levels of human decorin in the heart 10 days post-MI. Although decorin treatment had no effect on TGF-β expression, it largely blocked the activation of Smad2

and Smad3. This finding, together with those of the aforementioned studies by others, suggests that inhibition of the TGF-β/Smad2/Smad3 pathway contributes substantially to the reduction in cardiac fibrosis, as well as the reduced apoptosis and increased proliferation seen among granulation tissue cells in decorin-treated mice. Collectively, these effects would be expected to alter infarct tissue geometry to reduce wall stress and suppress myocardial fibrosis, thereby mitigating post-MI cardiac remodeling and dysfunction.

Hao et al. (17) previously reported increased protein expression levels of Smad2 and 3 in the rat MI model, which may appear to be inconsistent with our results that revealed activation of Smad2 and Smad3, but not upregulation of them. The most important difference may be the timing of examination, as well as difference in species (rat vs. mouse), which caused apparent conflict between the studies; Hao et al. examined MI at 8 wk after the onset, while we used 10-day-old MI. Hao et al. actually found that endogenous decorin expression was stronger in the hearts with older infarction.

It was not unexpected that the decorin gene therapy showed beneficial effects on postinfarction hearts in a strikingly similar manner as the previously reported sTβRII gene therapy, because decorin is a natural inhibitor of TGF-β, while sTβRII competitively inhibits binding of TGF-β with the TGF-β receptor (37). Pathophysiological mechanisms were very similar between these two gene therapies, as discussed above. In the present study, however, we found that decorin could increase cell proliferation in postinfarction granulation tissue and elucidated the inhibitory effect of decorin on TGF-β downstream signaling activation.

Possible clinical implications and limitations. Rapid recanalization of the occluded coronary artery, which salvages ischemic myocardial cells, is the best clinical approach at present to treating acute MI. Unfortunately, most patients actually lose their chance for coronary reperfusion therapy because it is only effective if performed within hours after the onset of infarction (41). The present findings suggest a novel therapeutic strategy, applicable during the subacute stage of MI, that may mitigate chronic progressive heart failure in MI patients who missed their chance for coronary reperfusion during the acute stage. In addition, treatment with decorin may be more promising than the use of sTβRII, which simply inhibits TGF-β signaling, when considering its additive beneficial effects, such as anti-tumor metastasis actions (15, 40, 52).

However, safety of anti-decorin strategies has not been confirmed in humans. In addition, ethical consensus has not been established at all in the safety of a virus-mediated gene therapy. These issues should be resolved before clinical application of the anti-decorin gene therapy.

ACKNOWLEDGMENTS

We thank Hatsue Ohshika in Gifu University Graduate School of Medicine for technical assistance.

GRANTS

This study was supported, in part, by postdoctoral fellowship for foreign researchers (to L. Li), by the Japan Society for the Promotion of Science, and by a Research Grant from Gifu University.

REFERENCES

1. **Ashcroft GS, Yang X, Glick AB, Weinstein M, Letterio JL, Mizel DE, Anzano M, Greenwell-Wild T, Wahl SM, Deng C, Roberts AB.** Mice lacking Smad3 show accelerated wound healing and an impaired local inflammatory response. *Nat Cell Biol* 1: 260–266, 1999.
2. **Beltrami AP, Urbanek K, Kajstura J, Yan SM, Finato N, Bussani R, Nadal-Ginard B, Silvestri F, Leri A, Beltrami CA, Anversa P.** Evidence that human cardiac myocytes divide after myocardial infarction. *N Engl J Med* 344: 1750–1757, 2001.
3. **Bourassa MG, Gurné O, Bangdiwala SI, Ghali JK, Young JB, Rousseau M, Johnstone DE, Yusuf S.** Natural history and patterns of current practice in heart failure. *J Am Coll Cardiol* 22, *Suppl* A: 14A–19A, 1993.
4. **Bujak M, Ren G, Kweon HJ, Dobaczewski M, Reddy A, Taffet G, Wang XF, Frangogiannis NG.** Essential role of Smad3 in infarct healing and in the pathogenesis of cardiac remodeling. *Circulation* 116: 2127–2138, 2007.
5. **Burlew BS, Weber KT.** Connective tissue and the heart: functional significance and regulatory mechanisms. *Cardiol Clin* 18: 435–442, 2000.
6. **Chen SH, Chen XH, Wang Y, Kosai K, Finegold MJ, Rich SS, Woo SL.** Combination gene therapy for liver metastasis of colon carcinoma in vivo. *Proc Natl Acad Sci USA* 92: 2577–2581, 1995.
7. **Cheng W, Kajstura J, Nitahara JA, Li B, Reiss K, Liu Y, Clark WA, Krajewski S, Reed JC, Olivetti G, Anversa P.** Programmed myocyte cell death affects the viable myocardium after infarction in rats. *Exp Cell Res* 226: 316–327, 1996.
8. **Derynck R, Zhang YE.** Smad-dependent and Smad-independent pathways in TGF-beta family signalling. *Nature* 425: 577–584, 2003.
9. **Desmoulière A, Redard M, Darby I, Gabbiani G.** Apoptosis mediates the decrease in cellularity during the transition between granulation tissue and scar. *Am J Pathol* 146: 56–66, 1995.
10. **Deten A, Holzl A, Leicht M, Barth W, Zimmer HG.** Changes in extracellular matrix and in transforming growth factor beta isoforms after coronary artery ligation in rats. *J Mol Cell Cardiol* 33: 1191–1207, 2001.
11. **Doran JP, Howie AJ, Townend JN.** Detection of myocardial infarction by immunohistological staining for C9 on formalin fixed, paraffin wax embedded sections. *J Clin Pathol* 49: 34–37, 1996.
12. **Gabbiani G.** The myofibroblast in wound healing and fibrocontractive diseases. *J Pathol* 200: 500–503, 2003.
13. **Gheorghiade M, Bonow RO.** Chronic heart failure in the United States: a manifestation of coronary artery disease. *Circulation* 97: 282–289, 1998.
14. **Gheorghiade M, Sopko G, De Luca L, Velazquez EJ, Parker JD, Binkley PF, Sadowski Z, Golba KS, Prior DL, Rouleau JL, Bonow RO.** Navigating the crossroads of coronary artery disease and heart failure. *Circulation* 114: 1202–1213, 2006.
15. **Grant DS, Yenisey C, Rose RW, Tootell M, Santra M, Iozzo RV.** Decorin suppresses tumor cell-mediated angiogenesis. *Oncogene* 21: 4765–4777, 2002.
16. **Hamner JB, Ellison KJ.** Predictors of hospital readmission after discharge in patients with congestive heart failure. *Heart Lung* 34: 231–239, 2005.
17. **Hao J, Ju H, Zhao S, Junaid A, Scammell-La Fleur T, Dixon IM.** Elevation of expression of Smad2, 3, and 4, decorin and TGF-beta in the chronic phase of myocardial infarct scar healing. *J Mol Cell Cardiol* 31: 667–678, 1999.
18. **Heldin CH, Miyazono K, ten Dijke P.** TGF-beta signalling from cell membrane to nucleus through SMAD proteins. *Nature* 390: 465–471, 1997.
19. **Huang SS, Huang JS.** TGF-beta control of cell proliferation. *J Cell Biochem* 96: 447–462, 2005.
20. **Isaka Y, Akagi Y, Ando Y, Tsujie M, Sudo T, Ohno N, Border WA, Noble NA, Kaneda Y, Hori M, Imai E.** Gene therapy by transforming growth factor-beta receptor-IgG Fc chimera suppressed extracellular matrix accumulation in experimental glomerulonephritis. *Kidney Int* 55: 465–475, 1999.
21. **Jahanyar J, Joyce DL, Southard RE, Loebe M, Noon GP, Koerner MM, Torre-Amione G, Youker KA.** Decorin-mediated transforming growth factor-beta inhibition ameliorates adverse cardiac remodeling. *J Heart Lung Transplant* 26: 34–40, 2007.
22. **Jalil JE, Doering CW, Janicki JS, Pick R, Shroff SG, Weber KT.** Fibrillar collagen and myocardial stiffness in the intact hypertrophied rat left ventricle. *Circ Res* 64: 1041–1050, 1989.
23. **Jang CW, Chen CH, Chen CC, Chen JY, Su YH, Chen RH.** TGF-beta induces apoptosis through Smad-mediated expression of DAP-kinase. *Nat Cell Biol* 4: 51–58, 2002.
24. **Kaiser J.** Clinical research. Death prompts a review of gene therapy vector. *Science* 317: 580, 2007.

25. **Krusius T, Ruoslahti E.** Primary structure of an extracellular matrix proteoglycan core protein deduced from cloned cDNA. *Proc Natl Acad Sci USA* 83: 7683–7687, 1986.
26. **Levy D, Kenchaiah S, Larson MG, Benjamin EJ, Kupka MJ, Ho KK, Murabito JM, Vasan RS.** Long-term trends in the incidence of and survival with heart failure. *N Engl J Med* 347: 1397–1402, 2002.
27. **Li Y, Takemura G, Kosai K, Takahashi T, Okada H, Miyata S, Yuge K, Nagano S, Esaki M, Khai NC, Goto K, Mikami A, Maruyama R, Minatoguchi S, Fujiwara T, Fujiwara H.** Critical roles for the Fas/Fas ligand system in postinfarction ventricular remodeling and heart failure. *Circ Res* 95: 627–236, 2004.
28. **Li Y, Li J, Zhu J, Sun B, Branca M, Tang Y, Foster W, Xiao X, Huard J.** Decorin gene transfer promotes muscle cell differentiation and muscle regeneration. *Mol Ther* 15: 1616–1622, 2007.
29. **Lijnen PJ, Petrov VV, Fagard RH.** Induction of cardiac fibrosis by transforming growth factor-beta 1. *Mol Genet Metab* 71: 418–435, 2000.
30. **Marshall E.** Gene therapy death prompts review of adenovirus vector. *Science* 286: 2244–2245, 1999.
31. **Masuda H, Takakura Y, Hashida M.** Pharmacokinetics and disposition characteristics of recombinant decorin after intravenous injection into mice. *Biochim Biophys Acta* 1426: 420–428, 1999.
32. **McKay RG, Pfeffer MA, Pasternak RC, Markis JE, Come PC, Nakao S, Alderman JD, Ferguson JJ, Safian RD, Grossman W.** Left ventricular remodeling after myocardial infarction: a corollary to infarct expansion. *Circulation* 74: 693–702, 1986.
33. **Mizuguchi H, Kay MA.** A simple method for constructing E1- and E1/E4-deleted recombinant adenoviral vectors. *Hum Gene Ther* 10: 2013–2017, 1999.
34. **Nagata S.** Apoptosis by death factor. *Cell* 88: 355–365, 1997.
35. **Nakagawa M, Takemura G, Kanamori H, Goto K, Maruyama R, Tsujimoto A, Ohno T, Okada H, Ogino A, Esaki M, Miyata S, Li L, Ushikoshi H, Aoyama T, Kawasaki M, Nagashima K, Fujiwara T, Minatoguchi S, Fujiwara H.** Mechanisms by which late coronary reperfusion mitigates postinfarction cardiac remodeling. *Circ Res* 103: 98–106, 2008.
36. **Ogino A, Takemura G, Kanamori H, Okada H, Maruyama R, Miyata S, Esaki M, Nakagawa M, Aoyama T, Ushikoshi H, Kawasaki M, Minatoguchi S, Fujiwara T, Fujiwara H.** Amlodipine inhibits granulation tissue cell apoptosis through reducing calcineurin activity to attenuate postinfarction cardiac remodeling. *Am J Physiol Heart Circ Physiol* 293: H2271–H2280, 2007.
37. **Okada H, Takemura G, Kosai K, Li Y, Takahashi T, Esaki M, Yuge K, Miyata S, Maruyama R, Mikami A, Minatoguchi S, Fujiwara T, Fujiwara H.** Postinfarction gene therapy against transforming growth factor-beta signal modulates infarct tissue dynamics and attenuates left ventricular remodeling and heart failure. *Circulation* 111: 2430–2437, 2005.
38. **Okada H, Takemura G, Kosai K, Tsujimoto A, Esaki M, Takahashi T, Nagano S, Kanamori H, Miyata S, Li Y, Ohno T, Maruyama R, Ogino A, Li L, Nakagawa M, Nagashima K, Fujiwara T, Fujiwara H, Minatoguchi S.** Combined therapy with cardioprotective cytokine administration and antiapoptotic gene transfer in postinfarction heart failure. *Am J Physiol Heart Circ Physiol* 296: H616–H626, 2009.
39. **Pfeffer MA.** Left ventricular remodeling after acute myocardial infarction. *Annu Rev Med* 46: 455–466, 1995.
40. **Reed CC, Waterhouse A, Kirby S, Kay P, Owens RT, McQuillan DJ, Iozzo RV.** Decorin prevents metastatic spreading of breast cancer. *Oncogene* 24: 1104–1110, 2005.
41. **Reimer KA, Vander Heide RS, Richard VJ.** Reperfusion in acute myocardial infarction: effect of timing and modulating factors in experimental models. *Am J Cardiol* 72: 13G–21G, 1993.
42. **Rissanen TT, Ylä-Herttuala S.** Current status of cardiovascular gene therapy. *Mol Ther* 15: 1233–1247, 2007.
43. **Ruoslahti E.** Structure and biology of proteoglycans. *Annu Rev Cell Biol* 4: 229–255, 1988.
44. **Sam F, Sawyer DB, Xie Z, Chang DL, Ngoy S, Brenner DA, Siwik DA, Singh K, Apstein CS, Colucci WS.** Mice lacking inducible nitric oxide synthase have improved left ventricular contractile function and reduced apoptotic cell death late after myocardial infarction. *Circ Res* 89: 351–356, 2001.
45. **Santra M, Santra S, Zhang J, Chopp M.** Ectopic decorin expression up-regulates VEGF expression in mouse cerebral endothelial cells via activation of the transcription factors Sp1, HIF1alpha, and Stat3. *J Neurochem* 105: 324–337, 2008.
46. **Schönherr E, Sunderkötter C, Schaefer L, Thanos S, Grässel S, Oldberg A, Iozzo RV, Young MF, Kresse H.** Decorin deficiency leads to impaired angiogenesis in injured mouse cornea. *J Vasc Res* 41: 499–508, 2004.
47. **Shan K, Kurrelmeyer K, Seta Y, Wang F, Dibbs Z, Deswal A, Lee-Jackson D, Mann DL.** The role of cytokines in disease progression in heart failure. *Curr Opin Cardiol* 12: 218–223, 1997.
48. **Shi Y, Massagué J.** Mechanisms of TGF-beta signaling from cell membrane to the nucleus. *Cell* 113: 685–700, 2003.
49. **Singla DK, Lyons GE, Kamp TJ.** Transplanted embryonic stem cells following mouse myocardial infarction inhibit apoptosis and cardiac remodeling. *Am J Physiol Heart Circ Physiol* 293: H1308–H1314, 2007.
50. **Sun Y, Weber KT.** Infarct scar: a dynamic tissue. *Cardiovasc Res* 46: 250–256, 2000.
51. **Takemura G, Ohno M, Hayakawa Y, Misao J, Kanoh M, Ohno A, Uno Y, Minatoguchi S, Fujiwara T, Fujiwara H.** Role of apoptosis in the disappearance of infiltrated and proliferated interstitial cells after myocardial infarction. *Circ Res* 82: 1130–1138, 1998.
52. **Tran KT, Lamb P, Deng JS.** Matrikines and matricryptins: implications for cutaneous cancers and skin repair. *J Dermatol Sci* 40: 11–20, 2005.
53. **Weisman HF, Bush DE, Mannisi JA, Weisfeldt ML, Healy B.** Cellular mechanisms of myocardial infarct expansion. *Circulation* 78: 186–201, 1988.
54. **Yamaguchi Y, Mann DM, Ruoslahti E.** Negative regulation of transforming growth factor-beta by the proteoglycan decorin. *Nature* 346: 281–284, 1990.
55. **Yin FC.** Ventricular wall stress. *Circ Res* 49: 829–842, 1981.
56. **Zaman AK, French CJ, Schneider DJ, Sobel BE.** A profibrotic effect of plasminogen activator inhibitor type-1 (PAI-1) in the heart. *Exp Biol Med (Maywood)* 234: 246–254, 2009.

The Journal of Laryngology & Otology (2009), 123 (Suppl. S31), *24–29.*

doi:10.1017/S0022215109005040

Main Article

Efficacy of autologous fat injection laryngoplasty with an adenoviral vector expressing hepatocyte growth factor in a canine model

H Umeno, S Chitose, Y Murofushi*, K Kosai*, K Sato, A Kawahara†, T Nakashima

Abstract

Objective: The effectiveness of autologous fat injection laryngoplasty may be reduced by resorption of injected fat tissue. The aim of the present study was to clarify the efficacy of fat injection laryngoplasty using autologous fat plus a replication-defective adenoviral vector expressing hepatocyte growth factor, regarding reduction of injected fat tissue resorption.

Material and methods: Four female beagle dogs were used in this study. After sedation, a direct laryngoscope was introduced to enable visualisation of the larynx. In each dog, harvested autologous fat plus an adenoviral vector expressing hepatocyte growth factor was injected into the right true vocal fold, and harvested fat plus an adenoviral vector expressing no gene was injected into the left true vocal fold. A total laryngectomy was performed one year after the intracordal fat injection. Coronal sections of the resected whole larynges were made and the following parameters assessed using light and electron microscopy: size of fat area; number of vasculoendothelial cells surrounding adipocytes; and shape of injected adipocytes in the vocal fold.

Results: The fat area was significantly larger and the number of vasculoendothelial cells surrounding adipocytes significantly greater in the intracordal fat injection containing adenoviral vector expressing hepatocyte growth factor, compared with the control intracordal fat injection containing adenoviral vector expressing no gene. When viewed under electron microscopy, the injected adipocytes were observed to have grafted better in the intracordal fat injection with hepatocyte growth factor adenoviral vector, compared with the control intracordal fat injection with adenoviral vector expressing no gene.

Conclusions: Injection into the vocal fold of autologous fat containing an adenoviral vector expressing hepatocyte growth factor can reduce subsequent resorption of injected fat.

Key words: Autologous Fat Injection Laryngoplasty; Adenoviral Vector; Hepatocyte Growth Factor; Vasculoendothelial Cell; Adipocytes

Introduction

Fat injection laryngoplasty is a minimally invasive surgical procedure, compared with framework surgery (i.e. type one thyroplasty, arytenoid adduction surgery or arytenoid adduction surgery plus type one thyroplasty), for the treatment of patients with unilateral vocal fold paralysis. Moreover, fat injection laryngoplasty is reliable, has good long-term results and yields stable, satisfactory vocal function in comparison with framework surgery.[1,2]

However, fat injection laryngoplasty is often followed by resorption of the injected fat. A larger quantity of autologous fat than needed is often injected into the vocal fold in order to compensate for resorption. In a series of 71 patients undergoing fat injection laryngoplasty, only 70–80 per cent subsequently showed normal aerodynamic parameters and acoustic analysis.[3] In addition, if the patient's body mass index (BMI) is high, there are risks associated with resorption of injected fat tissue.[4] Therefore, it is desirable to reduce resorption of injected fat tissue following fat injection laryngoplasty.

The aim of the present study was to assess the efficacy of fat injection laryngoplasty using autologous fat plus a replication-defective adenoviral vector expressing hepatocyte growth factor, regarding reduction of subsequent injected fat tissue resorption. Hepatocyte growth factor is associated with tissue regeneration, mitogenesis, angiogenesis, anti-apoptosis and anti-fibrotic activities in various cells.[5,6] The introduction of hepatocyte growth factor was expected to stimulate angiogenesis and therefore to reduce resorption of injected fat tissue.

From the Departments of Otolaryngology-Head and Neck Surgery and †Pathology, Kurume University School of Medicine, Kurume, and the *Division of Gene Therapy and Regenerative Medicine, Department of Neuro-musculoskeletal Disorders, Kagoshima University Graduate School of Medical and Dental Sciences, Japan.

Material and methods

Recombinant adenoviral vectors

As described previously, we generated and prepared a replication-defective adenoviral vector expressing hepatocyte growth factor, and a control adenoviral vector expressing no gene. The former viral vector encoded human hepatocyte growth factor downstream of the transcriptional control of a modified chicken beta-actin promoter, with a cytomegalovirus immediate early enhancer.[7–9]

Animal studies

Intracordal injection of autologous fat plus adenoviral vector. The study was approved by the institutional animal research committee. Four female beagle dogs weighting 9.6 to 11.5 kg were used.

The four dogs were sedated with an initial intravenous injection of propofol (6 mg/kg), followed by maintenance administration of propofol (0.2 to 0.5 mg/kg per minute) during surgery.

A subcutaneous injection of buprenorphine hydrochloride (0.05 mg/kg) provided analgesia. Autologous fat was harvested from the abdominal subcutaneous fat tissue by liposuction. In two dogs, only 0.5 ml of autologous fat was harvested because they had little subcutaneous fat tissue. In the other two dogs, 1.0 ml autologous fat was harvested.

A direct laryngoscope was then introduced to enable visualisation of the larynx.

In two dogs, adenoviral vector expressing hepatocyte growth factor (4.6×10^9 particles) was injected into the right vocal fold, together with 0.5 ml autologous fat, via a 19 G needle designed for endolaryngeal microsurgery. Adenoviral vector expressing no gene (4.6×10^9 particles) was injected into the left vocal fold together with 0.5 ml autologous fat, as a control.

In the other two dogs, adenoviral vector expressing hepatocyte growth factor (4.6×10^9 particles) was injected into the right vocal fold together with 1.0 ml autologous fat. Adenoviral vector expressing no gene (4.6×10^9 particles) was injected into the left vocal fold together with 1.0 ml autologous fat, as a control.

Histopathological analysis. The four dogs were humanely sacrificed 12 months after the initial intracordal autologous fat injection. The whole larynges were removed and fixed in 10 per cent formalin and dehydrated in graded concentrations of ethanol.

The bilateral vocal folds of the removed larynges were sectioned in a coronal plane into four pieces and embedded in paraffin. Haematoxylin and eosin stain and factor VIII stain (N1505; Dako, Tokyo, Japan) were used for each section. Haematoxylin and eosin staining was used to investigate the size of the fat tissue injection area. Each fat tissue area was measured with a light microscope, using Win Foof photoanalytical software. In addition, the total fat tissue area of the four sections of each vocal fold was measured for each dog. We then compared the total fat tissue area of the 16 sections of all four dogs' right vocal folds with that of the 16 sections of all four dogs' left vocal folds, using the variance component model to evaluate correlation among eight repeated measures within each dog.

Factor VIII staining was used to investigate angiogenesis around adipocytes. The number of vasculoendothelial cells surrounding adipocytes was counted at five different sites in each section, under light microscopy ($\times 400$). The total number of vasculoendothelial cells at 80 sites within the right vocal folds of all four dogs was compared with that at 80 sites within the left vocal folds of all four dogs, using Poisson regression with generalized estimating equation (GEE) estimation in order to determine the correlation within each dog.

For scanning electron microscopy, small specimens of injected adipocytes within the vocal fold were fixed in 2.5 per cent glutaraldehyde at 4°C for 2 hours. After rinsing with cacodylate buffer solution, specimens were postfixed in 2 per cent osmium tetroxide with cacodylate buffer solution at 4°C for 2 hours. This was followed by dehydration in a graded series of ethanol, immersion in *tert*-butyl alcohol and drying by the *tert*-butyl alcohol freezing method. Specimens were then sputter-coated with gold and examined under a Hitachi S-800 scanning electron microscope (Hitachi, Tokyo, Japan). The shape of adipocytes from the right and left vocal folds was compared.

Results

Bilateral coronal sections of a canine larynx one year after injection of 1.0 ml autologous fat are shown in Figure 1. The size of the fat tissue area in the right vocal fold, with adenoviral vector expressing hepatocyte growth factor, appears large in comparison with that in the left vocal fold, with adenoviral vector expressing no gene (i.e. control). Table I compares the fat tissue areas for 16 sections of right vocal fold (receiving hepatocyte growth factor viral vector) versus 16 sections of left vocal fold (receiving control viral vector), for all four dogs. The fat tissue area in the right vocal fold was statistically wider than that in the left vocal fold.

Figure 2 shows vasculoendothelial cells surrounding adipocytes. More vasculoendothelial cells were observed in the right vocal fold than in the left vocal fold. Table II compares vasculoendothelial cell results for 80 sites in the right vocal fold (receiving hepatocyte growth factor viral vector) versus 80 sites in the left vocal fold (receiving control viral vector), for the four dogs. The total number of vasculoendothelial cells surrounding the adipocytes was significantly larger in sites injected with autologous fat plus adenoviral vector expressing hepatocyte growth factor, compared with sites injected with autologous fat plus control adenoviral vector expressing no gene.

Figure 3 shows scanning electron microscopy views of the right and left vocal folds. Adipocyte diameter was longer and adipocyte density greater in the right vocal fold (receiving adenoviral vector expressing hepatocyte growth factor), compared with the left

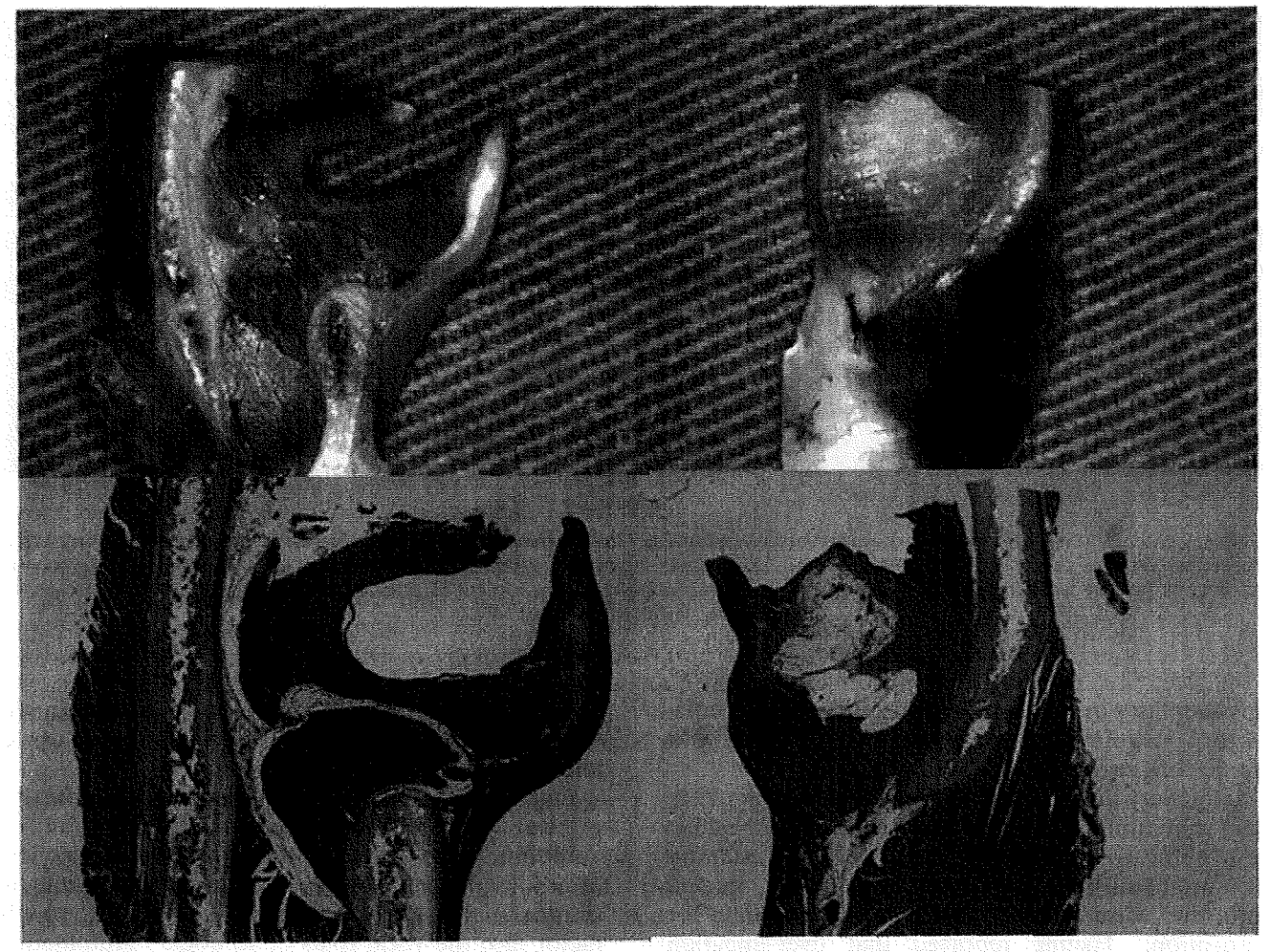

FIG. 1

(a) Coronal section of the right vocal fold (right) and left vocal fold (left). (b) Equivalent sections stained with H&E. The size of the fat tissue area in the right vocal fold (receiving adenoviral vector expressing hepatocyte growth factor) is wider than that in the left vocal fold (receiving adenoviral vector expressing no gene).

vocal fold (receiving adenoviral vector expressing no gene).

Discussion

Fat injection laryngoplasty was first reported by Mikaelian *et al.* in 1991.[10] This procedure is widely used because it appears to be a reasonable, safe alternative to framework surgery with high patient acceptance, which potentially offers long-term stability. Good results for the procedure have been reported by many authors.[11]

Furthermore, fat injection laryngoplasty is a minimally invasive procedure compared with framework surgery (i.e. type one thyroplasty, arytenoid adduction surgery, or arytenoid adduction surgery plus type one thyroplasty), for the treatment of patients with unilateral vocal fold paralysis. Fat injection

TABLE I

VOCAL FOLD FAT TISSUE AREA BY VIRAL VECTOR TYPE, FOR INDIVIDUAL AND COMBINED DOGS

Viral vector type	Fat tissue area (pixels/inch^2)		Test value (df)	p
	Mean	SD		
*1 dog**				
Ad.CA-HGF	1 866 234	976 880	3.21075 (3)	<0.049†
Ad.dE1.3	308 322	9947		
4 dogs‡				
Ad.CA-HGF	466 558	325 597	6.01 (3)	<0.0092**
Ad.dE1.3	77 081	46 908		

*Total of 20 sites (five sites in each of four coronal laryngeal sections). ‡Total of 80 sites (five sites in each of four coronal laryngeal sections, for four dogs). †Paired t-test; **t-test based on variance component model. Df = degrees of freedom; SD = standard deviation; Ad.CA-HGF = adenoviral vector expressing HGF (used in right vocal fold); Ad.dE1.3 = adenoviral vector expressing no gene (used in left vocal fold)

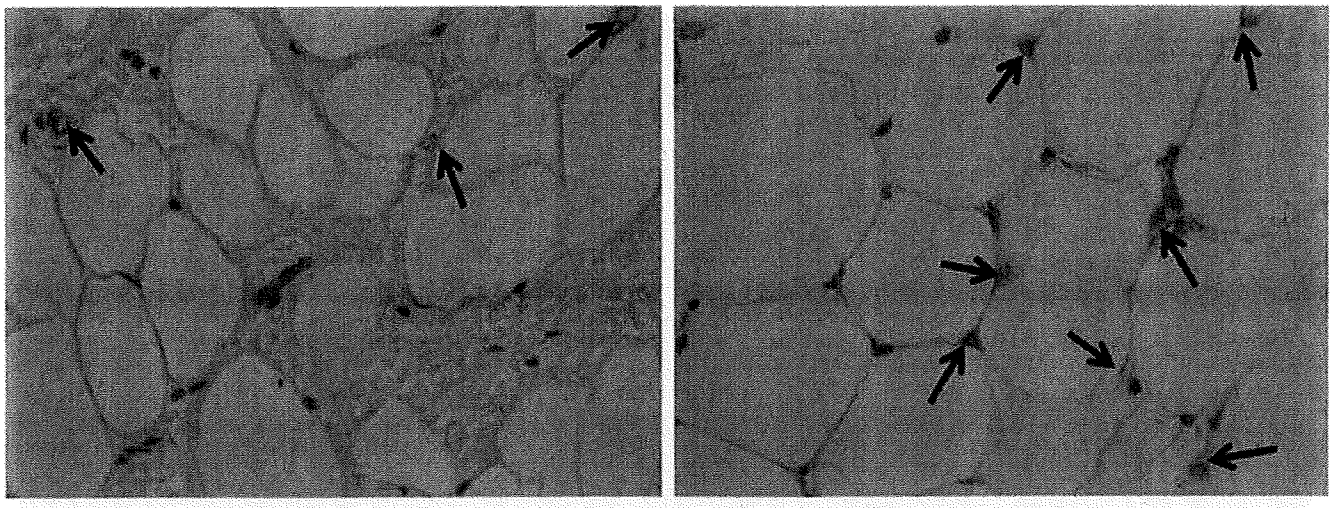

FIG. 2

Light microscopy photomicrographs showing vasculoendothelial cells (arrow) surrounding adipocytes in (a) the right vocal fold (receiving autologous fat plus adenoviral vector expressing hepatocyte growth factor) and (b) the left vocal fold (receiving autologous fat plus adenoviral vector expressing no gene). More vasculoendothelial cells were observed in the right vocal fold compared with the left vocal fold.

laryngoplasty has been found to result in more satisfactory post-operative vocal function, compared with framework surgery.[2]

However, autologous fat injection laryngoplasty can sometimes be associated with post-operative resorption of injected fat tissue. A larger quantity of autologous fat than needed is often injected into the vocal fold in order to compensate for resorption.[3] Hsiung reported that over-injection is necessary in order to medialise the vocal fold and to compensate for the anticipated fat absorption.[11]

In a series of 71 patients receiving fat injection laryngoplasty, 70–80 per cent subsequently showed normal aerodynamic parameters and acoustic analysis.[3] While these results are acceptable, there is room for improvement. Furthermore, post-operative resorption of injected fat tissue carries extra risks in patients with a high BMI.[4] Therefore, it is desirable to reduce the resorption rate of injected fat tissue after fat injection laryngoplasty.

TABLE II

VOCAL FOLD VASCULOENDOTHELIAL CELLS (SURROUNDING ADIPOCYTES) BY VIRAL VECTOR TYPE, FOR INDIVIDUAL AND COMBINED DOGS

Viral vector type	Vasculoendothelial cells (n/high power field)		χ^2 (df)	p
	Mean	SD		
*1 dog**				
Ad.CA-HGF	134.8	12.0	238.17 (1)	<0.001†
Ad.dE1.3	76.8	11.1		
4 dogs‡				
Ad.CA-HGF	33.7	5.9	238.41 (1)	<0.001†
Ad.dE1.3	19.2	5.2		

*Total of 20 sites (five sites in each of four coronal laryngeal sections for one dog). ‡Total of 80 sites (five sites in each of four coronal laryngeal sections, for four dogs). †Chi-square test based on Poisson model. Df = degrees of freedom; SD = standard deviation; Ad.CA-HGF = adenoviral vector expessing HGF (used in right vocal fold); Ad.dE1.3 = adenoviral vector expressing no gene (used in left vocal fold)

One study has addressed this issue. In an effort to prevent loss of fat volume and generation of additional adipose tissue after intracordal injection of autologous fat, Tamura *et al.* reported the effects of injecting fat together with basic fibroblast growth factor into the vocal folds of 12 dogs.[12] Autologous fat was injected into one vocal fold, and a mixture of autologous fat and gelatin microspheres containing basic fibroblast growth factor and collagen sponge was injected into the other. The vocal folds receiving autologous fat with basic fibroblast growth factor showed fusiform, immature adipocytes in the injected fat eight weeks after injection. The volume of the injected fat was maintained almost completely, even at 24 weeks post-injection. In comparison, the vocal folds receiving only autologous fat showed a marked decrease in the volume of injected fat over time. These results showed that strong vascularisation, occurring in response to basic fibroblast growth factor, prevents the loss of fat volume and the generation of additional adipose tissue, following intracordal injection of autologous fat.

Hepatocyte growth factor was originally identified and cloned as a potent mitogen for hepatocytes.[13,14] It has been reported to have mitogenic, angiogenic, antiapoptotic and antifibrotic effects on various cells.[5,6]

In the current study, hepatocyte growth factor was expected to stimulate angiogenesis around the injected fat tissue in the vocal fold. As expected, the number of vasculoendothelial cells surrounding adipocytes was significantly increased by the addition of hepatocyte growth factor. We surmise that the adipocytes were well supported by such increased vasculature. Furthermore, a large quantity of fat tissue was satisfactorily maintained in association with this

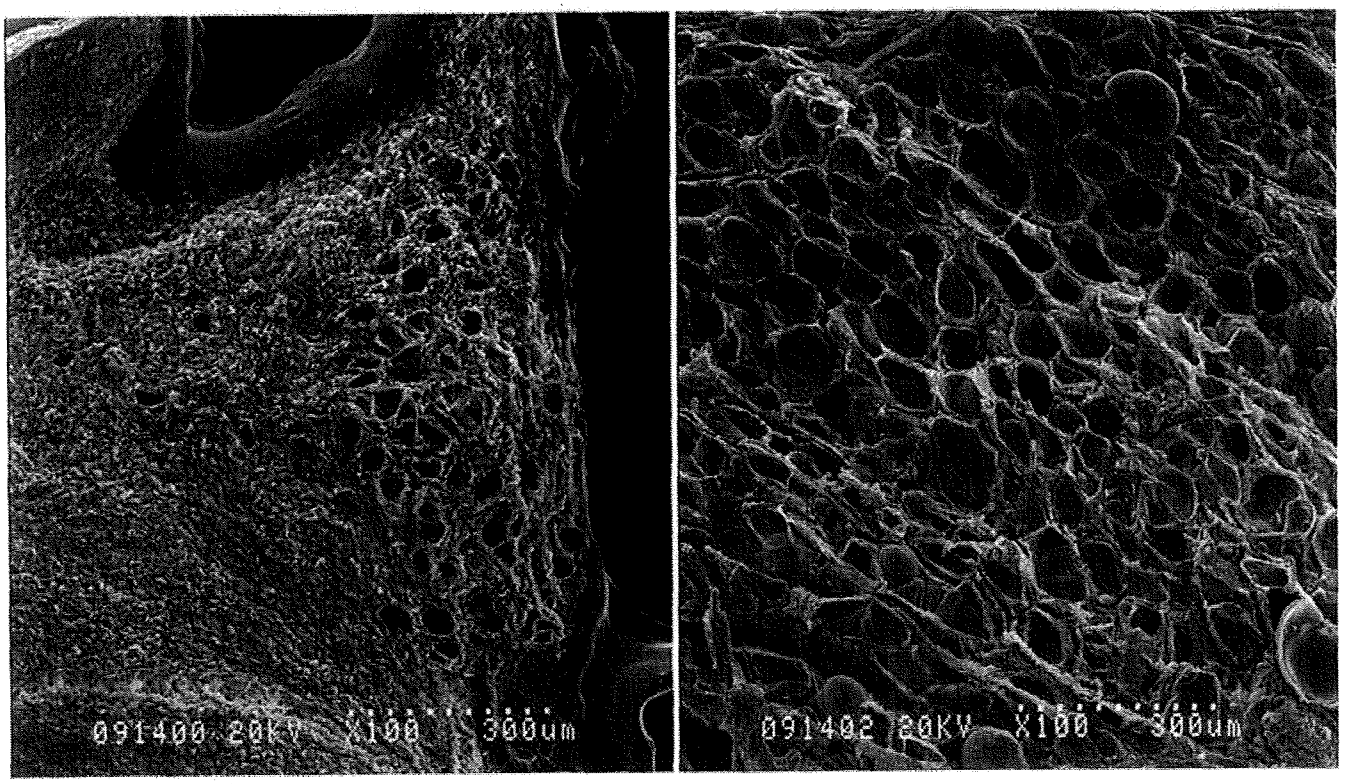

FIG. 3

Fig. 3 Scanning electron microscopy views of injected adipocytes in the (a) right and (b) left vocal folds. Adipocyte diameter and density were greater in the right vocal folds (receiving adenoviral vector expressing hepatocyte growth factor), compared with the left vocal folds (receiving adenoviral vector expressing no gene).

angiogenesis. As a result, the diameter and density of adipocytes were greater in the right vocal fold, which had received adenoviral vector expressing hepatocyte growth factor, compared with the left vocal fold, which had received only control adenoviral vector.

Gene therapy has been explored recently in the context of regenerative medical practice. Such efforts are based fundamentally on the expression of viral vectors to provide sustained release of a specific growth factor from cells using plasmid deoxyribonucleic acid have resulted in lower gene expression in comparison to viral vectors.

Cell transplantation therapy strategy in combination with growth factor has been recently explored in experiments in the context of regenerative medicine, and such previous efforts used administration of recombinant protein or plasmid DNA containing transgene. Although growth factor enhanced beneficial effects of cell transplantation therapy, the crucial issues in the previous approaches are short duration of half-lives of growth factor itself (*e.g.*, a few minutes in the body) and plasmid deoxyribonucleic acid (*e.g.*, a few days), as well as low transduction efficiency and low expression levels in the case of the use of plasmid DNA. In the present study, we for the first time used adenoviral vector system, which usually allows much higher gene transduction efficiency and much longer transgene expression (*e.g.*, several weeks), for introducing growth factor gene into the transplanted cells; in actuality, the present result was promising. In this regard, the novel strategy shown in this study may open up a new way in the field of cell transplantation therapy and regenerative medicine.

Conclusion

This study demonstrated the efficacy of fat injection laryngoplasty using autologous fat plus an adenoviral vector expressing hepatocyte growth factor, in a canine model. However, further preclinical study is necessary in order to carefully assess the clinical applicability of such treatment, including its safety and efficacy.

Acknowledgement

This study was supported in part by a Grant-in-Aid for Scientific Research (#19591997) from the Ministry of Education, Culture, Sports Science and Technology, Japan.

References

1 Umeno H, Shirouzu H, Chitose S, Nakashima T. Analysis of voice function following autologous fat injection for vocal fold paralysis. *Otolaryngol Head Neck Surg* 2005; **132**:103–7
2 Umeno H, Sato K, Shirouzu H, Chitose S, Nakashima T. Current state and future of autologous fat injection laryngoplasty – based on voice comparison between autologous fat injection laryngoplasty and framework surgery [in Japanese]. *Jpn J Logop Phoniatr* 2007;**48**:163–70
3 Umeno H, Sato K, Shirouzu H, Chitose S, Nakashima T. Fundamental and clinical medicine for fat injection laryngoplasty [in Japanese]. *Larynx Jpn* 2006;**18**:89–95
4 Sato K, Umeno H, Nakashima T. Histological investigation of liposuctioned fat for injection laryngoplasty. *Am J Otolaryngol* 2005;**26**:219–25

5 Matsumoto K, Nakamura T. Hepatocyte growth factor (HGF) as a tissue organizer for organogenesis and regeneration. *Biochem Biophys Res Commun* 1997;**239**:639–44
6 Birchmeier C, Gherardi E. Developmental roles of HGF/SF and its receptor, the c-Met tyrosine kinase. *Trends Cell Biol* 1998;**8**:404–10
7 Li Y, Takemura G, Kosai K, Yuge K, Nagano S, Esaki M *et al.* Postinfarction treatment with an adenoviral vector expressing hepatocyte growth factor relieves chronic left ventricular remodeling and dysfunction in mice. *Circulation* 2003;**107**:2499–506
8 Yuge K, Takahashi T, Nagano S, Terazaki Y, Murofushi Y, Ushikoshi H, Kawai T, Khai NC, Nakamura T, Fujiwara H, Kosai K. Adenoviral gene transduction of hepatocyte growth factor elicits inhibitory effects for hepatoma. *Int J Oncol* 2005;**27**:77–85
9 Murofushi Y, Nagano S, Kamizono J, Takahashi T, Fujiwara H, Komiya S, Matsuishi T, Kosai K. Cell cycle-specific changes in hTERT promoter activity in normal and cancerous cells in adenoviral gene therapy: A promising implication of telomerase-dependent targeted cancer gene therapy. *Int J Oncol* 2006;**29**:681–8
10 Mikaelian DO, Lowry LD, Sataloff RT. Lipoinjection for unilateral vocal cord paralysis. *Laryngoscope* 1991;**101**:465–8
11 Hsiung MW, Pai LU. Autologous fat injection for glottic insufficiency: analysis of 101 cases and correlation with patient's self-assessment. *Acta Otolaryngol* 2006;**126**:191–6
12 Tamura E, Fukuda H, Tabata Y. Adipose tissue formation in response to basic fibroblast growth factor. *Acta Otolaryngol* 2007;**127**:1327–31
13 Nakamura T, Nawa K, Ichihara A. Partial purification and characterization of hepatocyte growth factor from serum of hepatectomized rats. *Biochem Biophys Res Commun* 1984;**122**:1450–9
14 Nakamura T, Nishizawa T, Hagiya M, Seki T, Shimonishi M, Sugimura A *et al.* Molecular cloning and expression of human hepatocyte growth factor. *Nature* 1989;**342**:440–3

Address for correspondence:
Dr Hirohito Umeno,
Department of Otolaryngology-Head and Neck Surgery,
Kurume University School of Medicine,
67 Asahi-machi,
Kurume 830-0011, Japan.

Fax: +81 942 37 1200
E-mail: umeno2@med.kurume-u.ac.jp

Dr H Umeno takes responsibility for the integrity of the content of the paper.
Competing interests: None declared

Am J Physiol Heart Circ Physiol 296: H616–H626, 2009.
First published January 16, 2009; doi:10.1152/ajpheart.01147.2008.

Combined therapy with cardioprotective cytokine administration and antiapoptotic gene transfer in postinfarction heart failure

Hideshi Okada,[1] Genzou Takemura,[1] Ken-ichiro Kosai,[2] Akiko Tsujimoto,[1] Masayasu Esaki,[1] Tomoyuki Takahashi,[1] Satoshi Nagano,[1] Hiromitsu Kanamori,[1] Shusaku Miyata,[1] Yiwen Li,[1] Takamasa Ohno,[1] Rumi Maruyama,[1] Atsushi Ogino,[1] Longhu Li,[1] Munehiro Nakagawa,[1] Kenshi Nagashima,[1] Takako Fujiwara,[3] Hisayoshi Fujiwara,[1] and Shinya Minatoguchi[1]

[1]*Division of Cardiology, Graduate School of Medicine, Gifu University, Gifu;* [2]*Department of Structural Cell Biology, Graduate School of Medicine and Dental Sciences, Kagoshima University, Kagoshima; and* [3]*Department of Food Science, Kyoto Women's University, Kyoto, Japan*

Submitted 29 October 2008; accepted in final form 9 January 2009

Okada H, Takemura G, Kosai K, Tsujimoto A, Esaki M, Takahashi T, Nagano S, Kanamori II, Miyata S, Li Y, Ohno T, Maruyama R, Ogino A, Li L, Nakagawa M, Nagashima K, Fujiwara T, Fujiwara H, Minatoguchi S. Combined therapy with cardioprotective cytokine administration and antiapoptotic gene transfer in postinfarction heart failure. *Am J Physiol Heart Circ Physiol* 296: H616–H626, 2009. First published January 16, 2009; doi:10.1152/ajpheart.01147.2008.—We hypothesized that therapy, composed of antiapoptotic soluble Fas (sFas) gene transfer, combined with administration of the cardioprotective cytokine granulocyte colony-stimulating factor (G-CSF), would markedly mitigate cardiac remodeling and dysfunction following myocardial infarction (MI). On the 3rd day after MI induced by ligating the left coronary artery in mice, four different treatments were initiated: saline injection (Group C, $n = 26$); G-CSF administration (Group G, $n = 27$); adenoviral transfer of sFas gene (Group F, $n = 26$); and the latter two together (Group G+F, $n = 26$). Four weeks post-MI, Group G+F showed better survival than Group C (96 vs. 65%, $P < 0.05$) and the best cardiac function among the four groups. In Group G, the infarct scar was smaller and less fibrotic, whereas in Group F the scar was thicker, without a reduction in area, and contained abundant myofibroblasts and vascular cells; Group G+F showed both phenotypes. G-CSF exerted a beneficial effect on infarct tissue dynamics through antifibrotic and proliferative effects on granulation tissue; however, it also exerts an adverse proapoptotic effect that leads to thinning of the infarct scar. sFas appeared to offset the latter drawback. In vitro study using cultured myofibroblasts derived from the infarct tissue revealed that G-CSF increased proliferating activity of those cells accompanying activation of Akt and signal transducer and activator of transcription 3, while accelerating Fas-mediated apoptosis with increasing Bax-to-Bcl-2 ratio. The results suggest that combined use of G-CSF administration and sFas gene therapy is a potentially powerful tool against post-MI heart failure.

apoptosis; cytokines; gene therapy; heart failure; ischemic heart disease

LARGE MYOCARDIAL INFARCTION (MI) causes severe chronic heart failure with unfavorable remodeling of the left ventricle (LV) that is characterized by a ventricular dilatation and diminished cardiac performance (29). Although the magnitude of acute MI, which can be determined within several hours after an attack (30), is the most critical determinant of subsequent heart failure, other factors, such as late death or hypertrophy of cardiomyocytes, fibrosis, and the expression of various cytokines, are also associated with progression of the disease (7, 19, 31, 35). Infarcted tissue is highly dynamic and shows remarkable changes during the course of healing: necrotic tissue is infiltrated by inflammatory cells during the acute stage of MI; granulation tissue forms during the subacute stage; and scar tissue forms during the chronic stage (33, 37). Most cellular components that infiltrate and proliferate within an infarct, including inflammatory and granulation tissue cells, disappear via apoptosis during the acute and subacute stages of MI (34). In that regard, our laboratory previously reported that inhibition of apoptosis among granulation tissue cells during the subacute stage alters infarct tissue dynamics, making the infarct scar thicker and rich in preserved cellular components (13, 17). Such effects mitigate the adverse remodeling and dysfunction otherwise seen during the chronic stage, most likely by diminishing wall stress. One approach to suppressing apoptosis among granulation tissue cells is delivery of a gene encoding soluble Fas (sFas), a competitive inhibitor of Fas (17).

Evidence suggests that granulocyte colony-stimulating factor (G-CSF), a hematopoietic cytokine, can alleviate postinfarction LV remodeling and heart failure (11, 18, 21, 28). Various mechanisms have been proposed for the beneficial effects of G-CSF on the infarcted heart, including regeneration of myocardium (28), acceleration of the healing process (21), direct protection of cardiomyocytes from apoptosis (11), protection of salvaged cardiomyocytes, and reduction of myocardial fibrosis (18). However, the effects of G-CSF on the infarct tissue itself, the cellular (nonmyocyte) dynamics in particular, have not been well described. Given that G-CSF is known to act as a growth factor on some nonhematopoietic cell types, in addition to myeloid progenitor cells and mature neutrophils (2), we previously postulated that G-CSF affects infarct tissue cell dynamics to alter the infarct tissue geometry. Bearing that in mind, in the present study, we tested the hypothesis that, by cooperatively affecting infarct tissue dynamics, antiapoptotic sFas gene transfer, combined with administration of the proliferation-inducing cytokine G-CSF, might mitigate post-MI cardiac remodeling and dysfunction more effectively than either individual therapy alone.

Address for reprint requests and other correspondence: G. Takemura, Division of Cardiology, Gifu Univ. Graduate School of Medicine, 1-1 Yanagido, Gifu 501-1194, Japan (e-mail: gt@gifu-u.ac.jp).

The costs of publication of this article were defrayed in part by the payment of page charges. The article must therefore be hereby marked "*advertisement*" in accordance with 18 U.S.C. Section 1734 solely to indicate this fact.

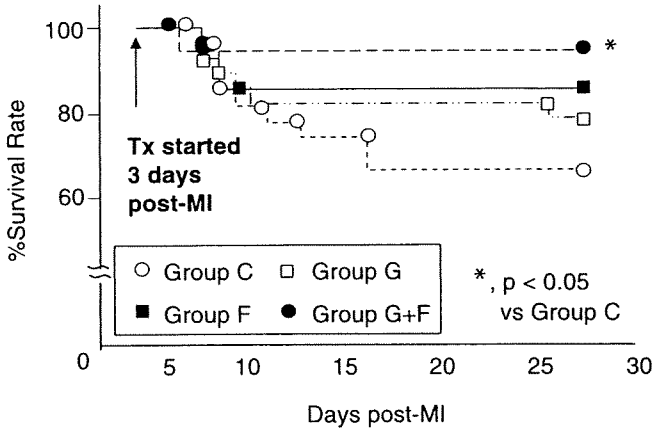

Fig. 1. Influence of the treatments (Tx) on post-myocardial infarction (MI) survival among mice followed up for 4 wk. ○, Group C; □, Group G; ■, Group F; ●, Group G+F. *$P < 0.05$ vs. Group C (Cox-Mantel log-rank test). See MATERIALS AND METHODS for explanation of groups.

MATERIALS AND METHODS

Recombinant adenoviral vectors. A replication-incompetent adenoviral vector that ubiquitously and strongly expresses a chimeric fusion protein composed of the extracellular region of mouse Fas and the Fc region of human IgG_1, i.e., sFas, was generated as follows. The adenoviral vector plasmid pAd-sFas, which is composed of the cytomegalovirus immediate early enhancer, a modified chicken β-actin promoter, rabbit β-globin polyA (CAG), and sFas cDNA (Ad.CAG-sFas), was constructed by in vitro ligation, as described previously (22). Control Ad-LacZ (Ad.CAG-LacZ) was prepared, as described previously (6).

We previously reported (17) that, in mice subjected to sFas gene delivery, the plasma levels of exogenous sFas measured 3 and 7 days after the injection (6 and 10 days post-MI) reached 51.0 ± 11.0 and 80.7 ± 4.7 μg/ml, respectively. At that point, the infarcted area was made up of granulation tissue (17), and these levels were thought to be high enough to exert a pharmacological effect, given that, in humans, the normal plasma sFas level is ~2 ng/ml (25).

Experimental protocols. This study conforms to the Guide for the Care and Use of Laboratory Animals published by the US National Institutes of Health (National Institutes of Health publication no. 85–23, revised 1996) and was approved by our Institutional Animal Research Committee. MI was induced in 130 male 10-wk-old C57BL/6J mice (Japan SLC) by ligating the left coronary artery, as previously described (17). On the 3rd day post-MI, the 105 surviving mice were randomly assigned into four groups. In Group G (G-CSF alone, $n = 27$), recombinant human G-CSF (lenograstim, Chugai Pharmaceutical) at the dose of 100 μg/kg was intraperitoneally injected once a day for 5 consecutive days. We determined the dose of G-CSF (100 μg/kg) based on previous studies reporting cardioprotective effects of G-CSF (11, 16). Although this dosage is extremely higher than the clinical dosage to humans (lower than 10 μg/kg), it is generally believed that mice have a low sensitivity to human G-CSF, as presumed by the unexpectedly poor increase in granulocytes. In Group F (Ad.CAG-sFas alone, $n = 26$), Ad.CAG-sFas (1×10^{11} particles/mouse) was injected into the hindlimb muscles. Group G+F (combination therapy, $n = 26$) received both treatments. In Group C (control, $n = 26$), Ad-LacZ and saline were injected. To avoid the influence of ischemic cardiomyocytes present during the acute stage of MI, we started the treatments on the 3rd day after the onset of MI. The mice were then followed up until 4 wk post-MI.

In a separate experiment, 40 mice were randomly assigned into the above four groups ($n = 10$ each) on the 3rd day post-MI, and the survivors ($n = 9$ in the combination group and $n = 7$ in the other groups) were killed 1 wk post-MI.

Cell culture. One week after inducing MI in mice, cardiac myofibroblasts were harvested from the infarcted areas of the hearts ($n = 3$) using a previously described method with some modification (17). Briefly, the heart was resected, and the infarcted area removed. The tissue was then minced and incubated with collagenase type II (Worthington) in Krebs-Ringer buffer for 30 min at 37°C. The dissociated cells were plated on 10-cm dishes for 1 h and then rigorously washed with buffer. The attached nonmyocytes that remained were cultured in DMEM supplemented with 5% FBS and were then used for experimentation during the second and third passages. More than 90% of the cells were found to be α-smooth muscle actin (SMA) positive.

In one experiment, the cells were incubated for 6 or 24 h in DMEM containing 5% FBS, with or without G-CSF (100 ng/ml); in another, a mixture of agonistic anti-Fas antibody (1 μg/ml, Pharmingen) and actinomycin D (0.05 μg/ml, Sigma) was applied for 6 or 24 h to induce apoptosis (24). In the latter experiments, we examined the effect of G-CSF (100 ng/ml) on Fas-mediated apoptosis. It is known that an additional treatment with a small dose of actinomycin D, a transcriptional inhibitor, is necessary to induce Fas-mediated apoptosis in several kinds of cells, such as hepatocytes, mesangeal cells, vascular smooth muscle cells, and cardiomyocytes in culture (1, 24). It was recently reported that the molecular mechanism involves upregulation of mitogen-activated protein kinase phosphatase-1, an inhibitor of c-Jun NH_2-terminal kinase (one of the key molecules of the Fas-induced apoptosis pathway), in cultured cardiomyocytes; this upregulation is inhibited by actinomycin D (1).

Physiological studies. Echocardiography and cardiac catheterization were performed before death, as previously described (23). Animals were anesthetized with halothane (induction, 2%; maintenance, 0.5%) in a mixture of N_2O and O_2 (0.5 l/min each) via a nasal

Table 1. *Cardiac function of the hearts 4 wk post-MI*

	Group C (Saline)	Group G (G-CSF)	Group F (sFas)	Group G+F (G-CSF + sFas)
n	17	21	22	25
Echocardiography				
LVDd, mm	5.7±0.3	5.2±0.1*	5.1±0.1*	4.5±0.1*†‡
Fractional shortening, %	12±1	20±1*	20±0.4*	23±0.5*†‡
Heart rate, beats/min	558±17	536±28	521±19	561±18
Cardiac catheterization				
LVSP, mmHg	53±5	80±2*	72±3*	70±3*
LVEDP, mmHg	12±2	5±1*	5±2*	3±1*†‡
+dP/d*t*, mmHg/s	2,682±402	3,954±332*	4,054±241*	4,929±198*†‡
−dP/d*t*, mmHg/s	−2,214±381	−3,357±308*	−3,327±224*	−3,965±139*

Values are means ± SE; *n*, no. of mice. G-CSF, granulocyte colony-stimulating factor; sFas, soluble Fas; LVDd, LV end-diastolic diameter; LVSP, LV peak systolic pressure; LVEDP, LV end-diastolic pressure; dP/d*t*, change in pressure over time. $P < 0.05$ compared with *Group C, †Group G, or ‡Group F (one-way ANOVA).

mask. Echocardiograms were recorded using an echocardiographic system (Vevo770, Visualsonics) equipped with a 45-MHz imaging transducer before treatment and at death. Following echocardiography, the right carotid artery was cannulated with a micromanometer-tipped catheter (SPR 671, Millar Instrument) that was advanced into the aorta and then into the LV for recording pressure and maximal and minimal change in pressure over time.

Histological analysis. After the physiological measurements were complete, all surviving mice were killed, and their hearts removed. Six hearts randomly chosen from each group were cut into two transverse slices, after which the basal specimens were fixed in 10% buffered formalin, embedded in paraffin, and cut into 4-μm-thick sections that were stained with hematoxylin-eosin, Masson's trichrome, and Sirius red F3BA (0.1% solution in saturated aqueous picric acid) (Aldrich). Quantitative assessments of the cell population and fibrotic area were performed in 20 randomly chosen high-power fields (HPF) in each section using a LUZEX F multipurpose color image processor (Nireco, Kyoto, Japan).

Immunohistochemical and immmunofluorescent analyses. Deparaffinized 4-μm-thick sections or 4% paraformaldehyde-fixed cultured cells were incubated first with a primary antibody against α-SMA (Sigma), Flk-1 (Santa Cruz), or Ki-67 (DAKO Japan). A Vectastain Elite ABC system (Vector Laboratories) was then used to label the sections; diaminobenzidine served as the chromogen, and the nuclei were counterstained with hematoxylin.

To double-label cultured cells, the cells were fixed with 4% paraformaldehyde and first incubated with primary antibodies against α-SMA and Ki-67, which were then respectively labeled with Alexa 568- and Alexa 488-conjugated secondary antibodies. Finally, the cells were counterstained with Hoechst 33342.

In situ DNA nick end-labeling [terminal deoxynucleotidyl transferase dUTP-mediated nick-end labeling (TUNEL)] assays were carried out with deparaffinized, 4-μm-thick sections using an ApopTag kit (Intergene), according to the supplier's instructions. For double TUNEL and immunofluorescent labeling of α-SMA in cultured cells, the cells were respectively labeled using Fluorescein-FragEL (Oncogene) and a primary antibody against α-SMA that was subsequently labeled with an Alexa 568-conjugated secondary antibody. In addition, to evaluate proliferative activity and apoptosis of cardiomyocytes, we performed double immunofluorescence myoglobin combined with Ki-67 or TUNEL. Tissue sections were first stained with anti-Ki-67 followed by Alexa 488 or Fluorescein-FragEL and then labeled with anti-myoglobin antibody (DAKO) followed by Alexa 568. Nuclei were stained with Hoechst 33342.

Western blotting. Proteins extracted from cardiac tissue (50 μg) or cultured cells (6 μg) were subjected to 14% polyacrylamide gel electrophoresis and then transferred onto polyvinylidene difluoride membranes. The membranes were then probed using primary antibodies against matrix metalloproteinase-2 (MMP-2, Daiichi Fine Chemical), MMP-9 (Santa Cruz), extracellular signal-regulated kinase (ERK), phosphorylated (activated) form of ERK, Akt, phosphorylated form of Akt, signal transducer and activator of transcription 3 (Stat3), the phosphorylated form of Stat3 (all from Cell Signaling), Bcl-2, or Bax (both from Santa Cruz), after which the blots were visualized using chemiluminescence (ELC, Amersham), and the signals were quantified by densitometry (NIH IMAGE 1.63). α-Tubulin (analyzed using an antibody from Santa Cruz) or β-actin (antibody from Sigma) served as the loading control. Samples of $n = 5$ or 6 from each group were subjected to Western blotting.

Electron microscopy. After excising the hearts, cardiac tissue was quickly cut into 1-mm cubes, immersion fixed in 2.5% glutaraldehyde in 0.1 mol/l phosphate buffer (pH 7.4) overnight at 4°C, and postfixed in 1% buffered osmium tetroxide. The specimens were then dehydrated through a graded ethanol series and embedded in epoxy resin. Ultrathin sections (90 nm), double-stained with uranyl acetate and lead citrate, were examined under an electron microscope (H-800, Hitachi).

Statistical analysis. Values are shown as means ± SE. Analyses of survival were carried out using the Kaplan-Meier method; significant differences were determined using the log-rank test (Cox-Mantel). The significance of differences between groups was evaluated using *t*-tests or one-way ANOVA with a post hoc Newman-Keul's multiple-comparisons test. Values of $P < 0.05$ were considered significant.

RESULTS

Survival, cardiac function, and cardiac histology at the chronic stage of MI. As shown in Fig. 1, the survival rate 4 wk post-MI was 65% (17 of 26 mice) in Group C, 78% (21 of 27 mice) in Group G, 85% (22 of 26 mice) in Group F, and 96% (25 of 26 mice) in Group G+F. The survival rate among mice in Group G+F was significantly better than among those in Group C.

Echocardiography and cardiac catheterization revealed that, 4 wk post-MI, the control mice in Group C showed severe LV

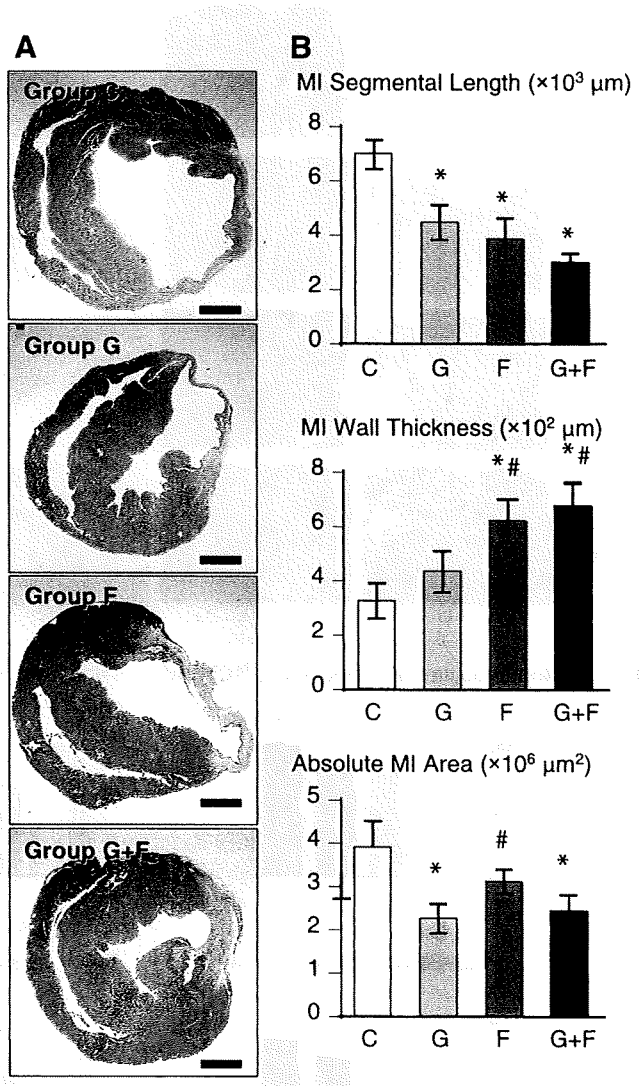

Fig. 2. Effect of the treatments on ventricular remodeling and infarct geometry during the chronic stage of MI (4 wk post-MI). *A*: transverse sections of hearts stained with Masson's trichrome. Bars = 1 mm. *B*: graph showing the length of the infarct segment (outer circumferential length, μm), the thickness of the infarct wall (μm), and the absolute infarct area (μm²) in each group. *$P < 0.05$ vs. Group C, #$P < 0.05$ vs. Group G (one-way ANOVA).

remodeling with marked enlargement of the LV cavity and signs of reduced cardiac function: decreased LV %fractional shortening and maximal and minimal change in pressure over time and increased LV end-diastolic pressure (Table 1). Although post-MI cardiac dysfunction and remodeling were mitigated significantly in Groups G and F, they were reduced to a significantly greater degree in Group G+F than in the other two treatment groups.

There was no significant difference in heart weight or in the heart-to-body weight ratios among the groups. Compared with control hearts with 4-wk-old MIs (Group C), which showed marked LV dilatation with a thin infarct segment, the LV cavity in hearts from the treated groups were smaller (Fig. 2). In addition, the absolute area of the infarct scar was significantly smaller in hearts from Groups G and G+F than in those from Groups C and F. The circumferential length of the infarct segment was significantly shorter, while the infarct wall was significantly thicker in all treated groups than in Group C (Fig. 2).

In Group C, the infarct area was replaced with dense fibrous tissue with a scanty cell component 4 wk post-MI. In the treated groups, by contrast, the infarct area appeared to contain a greater cellular component (Fig. 3). Morphometric analysis of Sirius red-stained preparations confirmed there to be less fibrosis and a greater cell population in the treated groups, among which Group G+F showed the largest cellular component (Fig. 3). The %area of extravascular α-SMA-positive cells (myofibroblasts) was greatest in Group G+F and greater in Group F than in Group C or G. Some α-SMA-positive cells accumulated and formed bundles that were not observed in the

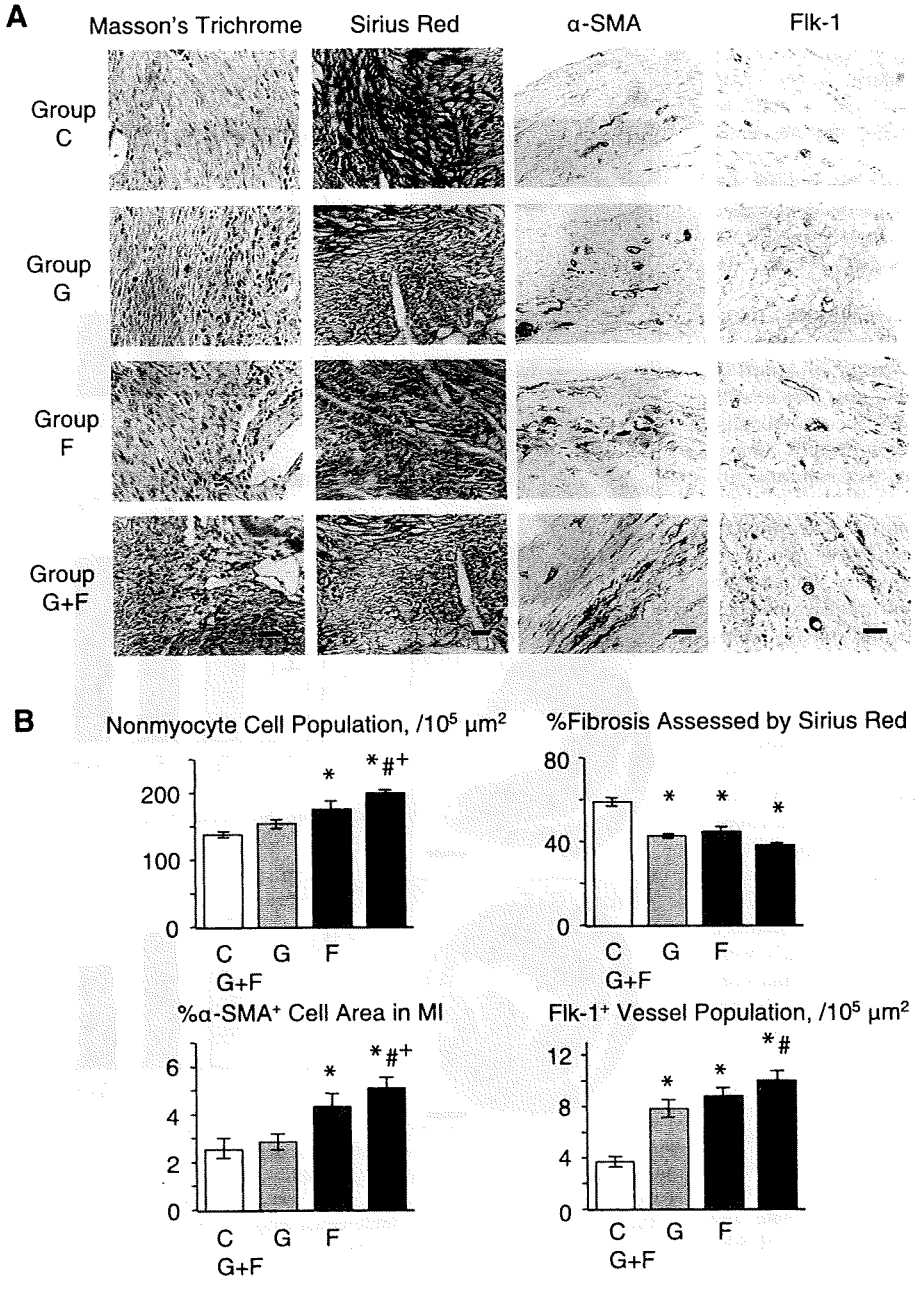

Fig. 3. Effect of the treatments on the 4-wk-old infarct tissue histology. *A*: photomicrographs of infarcted areas from mouse hearts collected 4 wk post-MI. Bars, 20 μm. *B*: graphs showing the nonmyocyte cell population, %fibrosis, %area of the α-smooth muscle actin (SMA)-positive myofibroblasts, and population of Flk-1-positive vessels in infarct tissue of each group. $^{*}P < 0.05$ vs. Group C, $^{\#}P < 0.05$ vs. Group G, $^{+}P < 0.05$ vs. Group F (one-way ANOVA).

infarcted wall of the control mice (Fig. 3). The numbers of Flk-1-positive vessels were higher in all treated groups than in Group C, and the numbers in Group G+F were even higher than in Group G (Fig. 3).

As we detected less fibrosis in the G-CSF-, sFas gene-, or both treated hearts than the control hearts, we examined expression of MMP-2 and -9. Western blot analysis showed that both MMP-2 and -9 were significantly overexpressed in the hearts administered G-CSF, compared with untreated hearts and sFas gene alone-treated hearts (Fig. 4).

Granulation tissue cell dynamics at the subacute stage. We next examined groups of hearts with 1-wk-old MIs to evaluate granulation tissue cell proliferation and apoptosis. Modulation of these processes by the present treatments could explain the observed histological differences (nonmyocyte population in particular) in the infarct scars at the chronic stage of MI. Numbers of proliferating cells, which were identified based on their Ki-67-positive nuclei, were significantly higher in hearts treated with G-CSF (210 ± 6 cells/HPF in Group G and 219 ± 14 cells/HPF in Group G+F) than in the other groups (92 ± 7 cells/HPF in Group C and 100 ± 9 cells/HPF in Group F) (Fig. 5*A*). Electron microscopy actually demonstrated proliferating cells in granulation tissue, as shown in Fig. 5*B*.

On the other hand, TUNEL assays showed that apoptosis among granulation tissue cells (160 ± 7 cells/HPF in Group C) was significantly suppressed by sFas gene transfer (113 ± 13 cells/HPF in Group F and 115 ± 8 cells/HPF in Group G+F), as expected. Somewhat unexpectedly, however, granulation tissue in Group G showed a significantly higher incidence of apoptosis (214 ± 15 cells/HPF) than that in Group C (Fig. 5*C*). Figure 5*D* shows an ultrastructural feature of granulation tissue cell apoptosis.

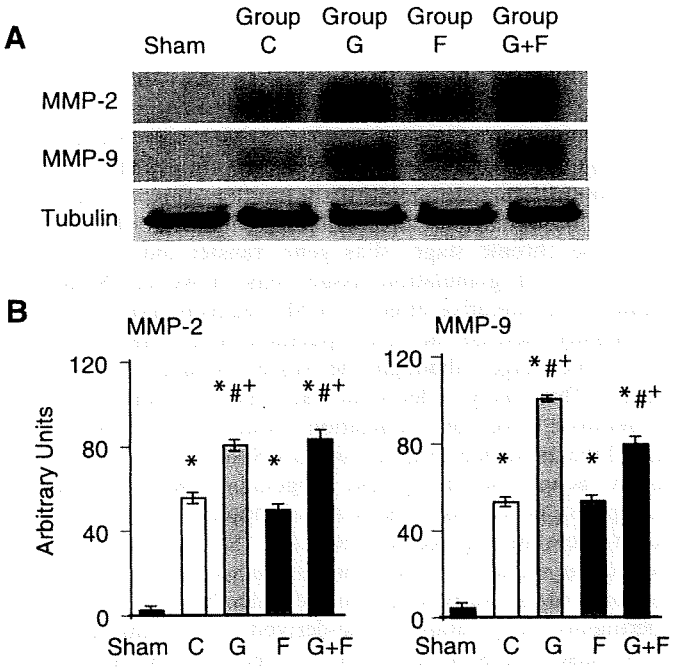

Fig. 4. Expression of matrix metalloproteinase (MMP)-2 and -9 in hearts with 4-wk old MI. *A*: Western blot showing myocardial expression of MMP-2 and -9 in each group. *B*: their quantification by densitometry. $^{*}P < 0.05$ vs. sham, $^{\#}P < 0.05$ vs. Group C, $^{+}P < 0.05$ vs. Group F (one-way ANOVA).

Effect of the treatments on viable myocardium. To check whether the treatment (with G-CSF in particular) promoted viable cardiomyocytes to replace the function of the infarcted area, we examined cell proliferation activity and apoptosis in viable myocardium. Double immunofluorescence for myoglobin and Ki-67 revealed no proliferating cardiomyocyte in viable myocardium of any groups at either 1 wk or 4 wk post-MI (photographs not shown). We noted TUNEL-positive cardiomyocytes in viable myocardium. However, they were extremely rare (~0.02%) in each group at either 1 wk or 4 wk post-MI, and there was no significant difference in the incidence among the groups at either stage (Fig. 6). These findings do not support the possibility that the present treatments increased regeneration or reduced cell loss due to apoptosis of viable cardiomyocytes to replace the infarcted area.

Effect of G-CSF on proliferation and apoptosis of infarct tissue-derived myofibroblasts. To confirm the in vivo findings summarized above, the proliferative and proapoptotic effects of G-CSF were examined in vitro using granulation tissue-derived cultured myofibroblasts. Addition of G-CSF (100 ng/ml) to the cells significantly increased the proliferation rate (%Ki-67-positive cells) among cultured myofibroblasts after incubation for 24 h: saline, 21 ± 2.2% vs. G-CSF, 36 ± 2.1% ($P < 0.05$) (Fig. 6*A*). As the binding of G-CSF to its receptor evokes signal transduction through activation of Janus kinase/Stat, Akt kinase, which has been identified as a downstream target of phosphatidylinositol-3′-kinase, and mitogen-activated protein kinase/ERK (2, 8), we next examined their activity. Western blotting using phosphorylated forms of ERK, Stat3, and Akt revealed that Stat3 and Akt, but not ERK, were significantly activated in the G-CSF-treated myofibroblasts (Fig. 6*B*).

However, we also noted that G-CSF increased the incidence of Fas-mediated apotosis: %TUNEL positivity among cells treated with Fas antibody plus actinomycin D was 42 ± 3.8%; upon addition of G-CSF to the Fas antibody plus actinomycin D, the incidence increased to 55 ± 3.2% (Fig. 7*A*; $P < 0.05$). The ratio of Bax to Bcl-2 determines death or survival after an apoptotic stimulus (27), and our Western blotting showed an increase of that ratio in the Fas-mediated apoptosis of cultured myofibroblasts (Fig. 7*B*). Interestingly, the increase of the ratio was more significant by the additional G-CSF treatment (Fig. 7*B*).

DISCUSSION

The present study confirmed that post-MI treatment with G-CSF or sFas gene transfer can individually mitigate cardiac dysfunction at the chronic stage (4 wk post-MI) (11, 17, 21). Moreover, we found that their combination further improves post-MI survival and elicits a more pronounced mitigation of post-MI cardiac dysfunction than was seen in groups receiving a single treatment. Although G-CSF administration and sFas gene transfer each improved cardiac function to a similar degree, the structures of the 4-wk-old infarct scars were substantially different in the two groups. Compared with Group C, the infarct scars in Group G were shorter in circumferential length and smaller in the area, while those in Group F were shorter and thicker but not smaller in area. This is noteworthy in that the segmental length of the infarct scar is an important determinant of adverse LV remodeling, directly contributing to

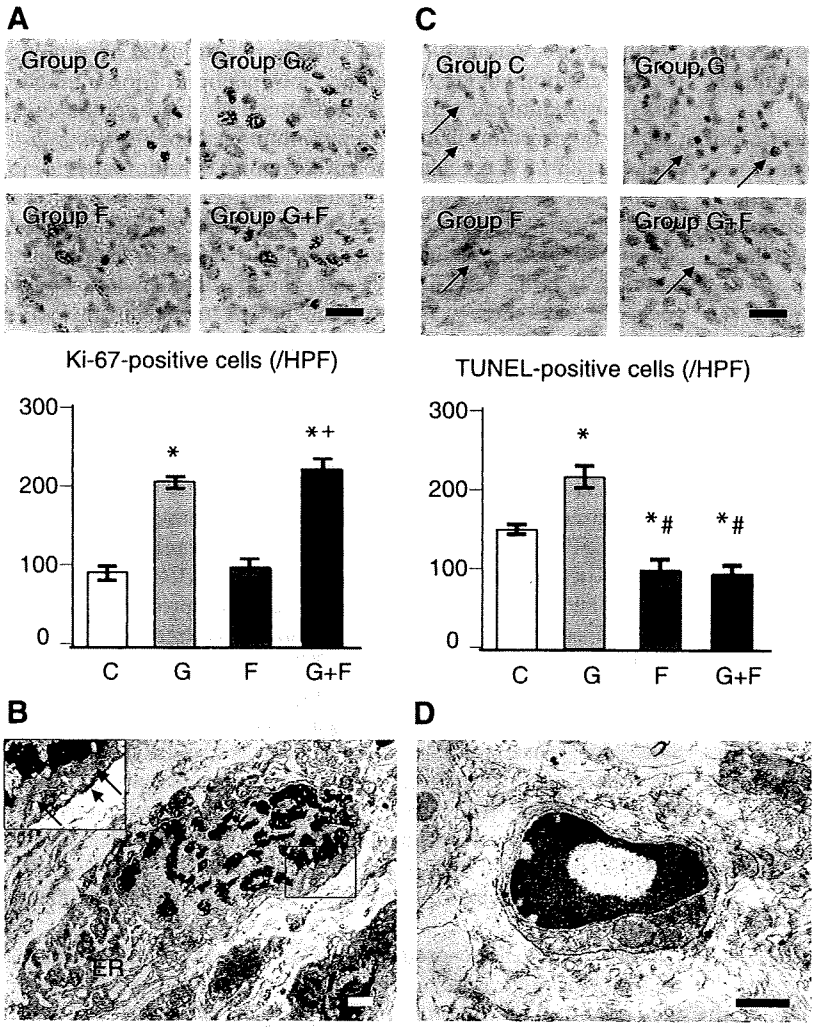

Fig. 5. Cell proliferation and apoptosis in granulation tissue cells of 1-wk old MI. *A*: photomicrographs show immunohistochemical preparations for Ki-67. Bar = 20 μm. The graph shows the incidence of Ki-67-positive cells in each group. *B*: electron photomicrograph of a proliferating myofibroblast in granulation tissue. Nuclear morphology indicates that the cell is at anaphase of mitosis. The cell type was ultrastructurally identified as a myofibroblast, presenting well-developed endoplasmic reticulum (ER) and scanty myofilaments (arrows in the *inset*) and dense body (arrowhead in the *inset*) at the periphery. This cell was from the heart of Group G+F. Bar = 1 μm. *C*: photographs show terminal deoxynucleotidyl transferase dUTP-mediated nick-end labeling (TUNEL)-stained preparations of the infarcted area of mouse hearts 1 wk post-MI. Arrows indicate TUNEL-positive cells. Bars = 20 μm. The graph shows the incidence of TUNEL-positive cells in each group. *D*: electron photomicrograph of an apoptotic granulation tissue cell, of which cell type is difficult to identify because of severe cytoplasmic shrinkage. This cell was from the heart of Group G. Bar = 1 μm. $^{*}P < 0.05$ vs. Group C, $\#P < 0.05$ vs. Group G, $^{+}P < 0.05$ vs. Group F (one-way ANOVA). HPF, high-power field.

LV dilatation. The wall thickness of infarct scars is also important because wall stress is proportional to the cavity diameter and inversely proportional to the wall thickness (Laplace's law) (38). Since wall stress and adverse LV remodeling (dilatation) have a vicious relationship in which they accelerate one another, it is easy to surmise that such an alteration in the geometry of the infarct would improve the hemodynamic state of the heart. In Group G+F, the infarct scar had a phenotype that combined the features of both Groups G and F, i.e., it was smaller, shorter, and thicker than control. This geometric advantage in Group G+F is likely an important element that prevents the worsening of cardiac dysfunction. We actually found more than 100% increase in MI wall thickness, despite an increase in nonmyocyte cell population of ~30% in Group G+F. Although dissociation in the extent of increase appears to be too much between the wall thickness and cell population, the wall thickness is determined not only by the cell population, but also by wall stress: when the MI wall is thinner, the wall stress becomes greater to make the wall more increasingly thinner. Thus it is surmised that even a slight increase of the MI wall by the increased cell population could have greatly prevented thinning of the MI wall in Group G+F. On the other hand, the present findings did not support a possibility of an increased cardiomyocyte population related to increased regeneration and/or reduced apoptosis by any treatments.

Confirming an earlier study (17), our laboratory found that an antiapoptotic strategy using sFas gene transfer prevented granulation tissue cell apoptosis during the subacute stage of MI and preserved the cell population within the infarct scar during the chronic stage. sFas gene transfer did not affect proliferation of granulation tissue cells, however. Notably, despite its proliferative effect, G-CSF treatment alone did not significantly increase the cell population in the infarct scar at the chronic stage, although the vessel population was increased. This likely reflects the fact that, in addition to its proliferative effect on granulation tissue, G-CSF also augmented the incidence of apoptosis. G-CSF is known to act as a growth factor toward myeloid progenitor cells and mature neutrophils, as well as some nonhematopoietic cell types (2), and to exert an angiogenic effect (4, 15). The proliferative effect on granulation tissue, which includes vascular cells, is, therefore, not so surprising. On the other hand, our in vitro experiments using infarct tissue-derived cells confirmed that G-CSF also exerts a proliferative effect on myofibroblasts accompanying activation of Stat3 and Akt. And even more unexpected was the proapoptotic effect of G-CSF on granulation tissue myofibroblasts. The in vitro study using Fas-stim-

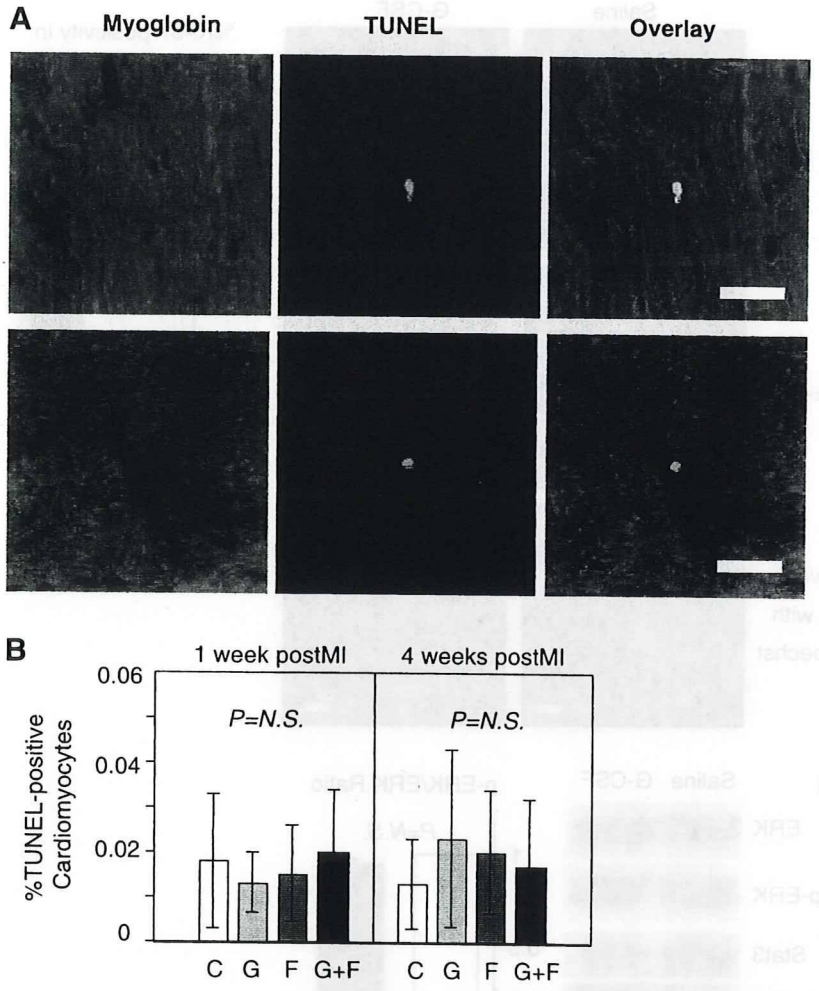

Fig. 6. Examination of apoptosis in viable myocardium. *A*: double immunofluorescence images for myoglobin (as a cardiomyocyte marker; red) and TUNEL (green) show a TUNEL-positive cardiomyocyte (*top*) and a TUNEL-positive noncardiomyocyte (*bottom*) in noninfarcted area of the untreated heart 1 wk post-MI. Nuclei were stained with Hoechst (blue). Bars, 10 μm. *B*: graph comparing the incidences of TUNEL-positive cardiomyocytes in noninfarcted area among the groups at 1 and 4 wk post-MI. There was no significant difference between the groups at either time point (one-way ANOVA). NS, nonsignificant.

ulated myofibroblasts confirmed this and also revealed further increase of Bax-to-Bcl-2 ratio by the additional treatment with G-CSF. Apoptotic loss of infarct tissue cells could cause thinning of the infarct wall, leading to an increase in wall stress. Moreover, myofibroblasts are well known to play an important role in wound contraction during the healing process (9) and also in infarct scar contraction (shortening) (13, 17, 26). Thus the effect of G-CSF on infarct tissue cell dynamics may be a double-edged sword. We suggest that, when administered in combination with G-CSF, sFas gene transfer offsets the potentially adverse (proapoptotic) effects of G-CSF (Fig. 8).

We found fibrosis to be significantly reduced in the infarct scars of all the treated groups. The improved wall mechanics seen in all three treatment groups would be expected to reduce fibrosis by reducing stretch, which is known to stimulate collagen production. The relative area of fibrosis within the infarct scar also would be reduced in the groups where the cellular components were well preserved and occupied a substantial area of the infarct scar (Groups F and G+F). In addition, G-CSF is known to induce expression of MMP-2 and MMP-9 (5, 18), and we confirmed this fact in the present study. Several fibrogenic factors, including tumor necrosis factor-α, transforming growth factor-β_1, and angiotensin II type 1 receptor were conversely downregulated in hearts with old MIs (18). These actions may have collectively contributed to reducing fibrosis in the infarct scars of hearts from Group G+F.

We noted TUNEL-positive cardiomyocytes in the 1- and 4-wk post-MI hearts, although in a rare incidence (~0.02%). The incidence of them was not affected either by G-CSF or sFas treatment (Fig. 9). Cardiomyocyte apoptosis has been suggested to be involved in the setting of MI at two different stages: *1*) acute death of the cardiomyocytes in the infarcted area just after reperfusion (several hours) (10); and *2*) late death of the salvaged cardiomyocytes during the subacute to chronic stages (days to weeks) (3). Our study has relevance to the latter case because the treatments were started on *day 3* of MI. Although a previous study reported an antiapoptotic effect of G-CSF on cardiomyocytes at the acute stage (11), that effect has not been demonstrated during the later stages of MI. The interaction of Fas with Fas ligand is an important trigger for apoptosis in many cell types, including cells related to the immune system and granulation tissue cells (17, 23). However, an adult cardiomyocyte is reportedly very insensitive to Fas-mediated apoptosis (12, 36).

The present study has several limitations. We delivered both G-CSF and sFas in a systemic fashion in the present study. It is enough of a possibility that systemically circulating G-CSF, sFas, or both would have activated extracardiac tissue or cells to indirectly affect the heart, e.g., through some other cell type,

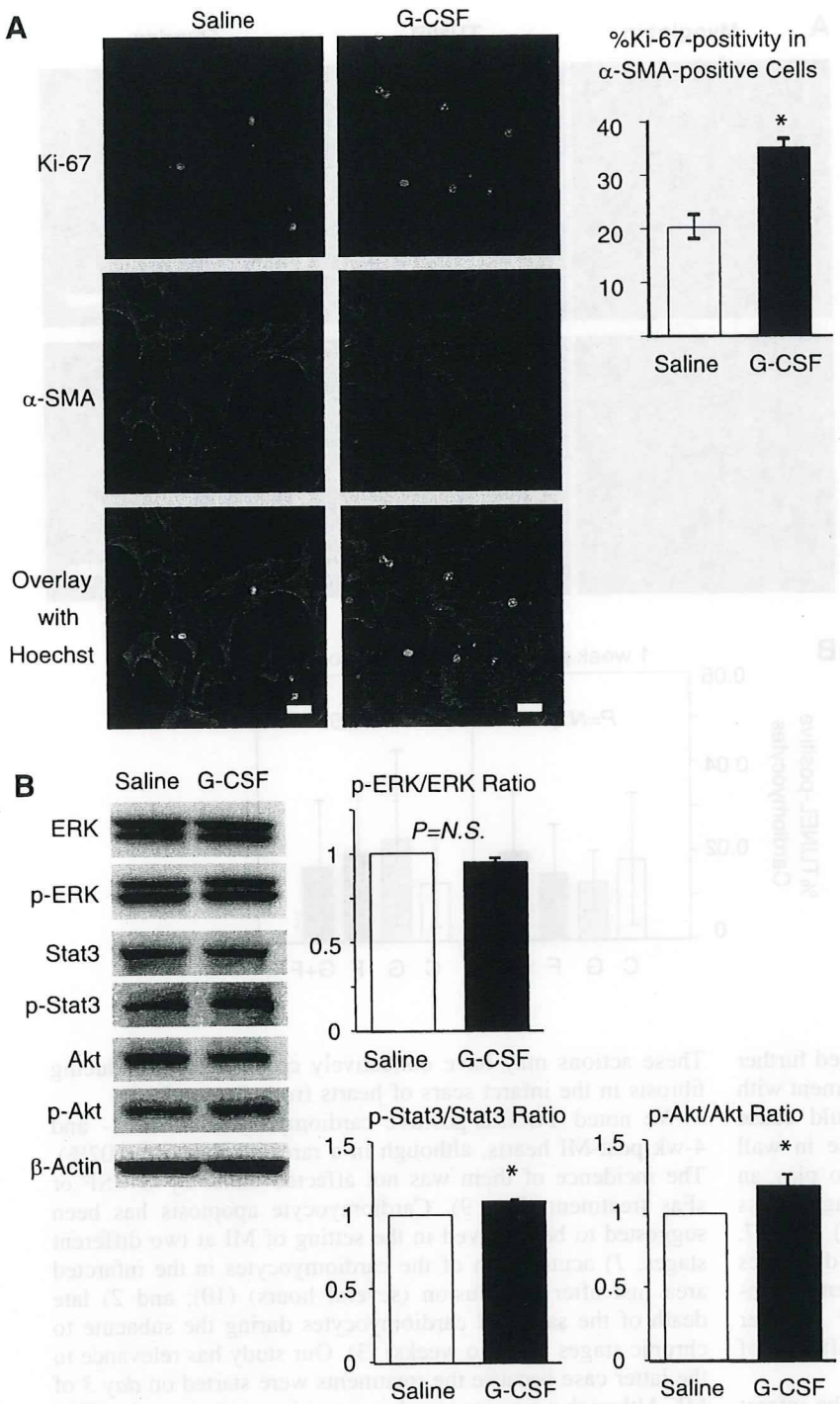

Fig. 7. In vitro effect of granulocyte colony-stimulating factor (G-CSF) on proliferation and the related signal activation among myofibroblasts. *A*: effect of G-CSF on proliferation of α-SMA-positive myofibroblasts derived from 1-wk-old infarct tissue assessed by Ki-67 immunofluorescence. Bars = 20 μm. The graph shows the %Ki-67-positivity among the cells. *B*: effect of G-CSF (100 ng/ml) on expression and activation of extracellular signal-regulated kinase (ERK), signal transducer and activator of transcription 3 (Stat3), and Akt in cultured myofibroblasts. $*P < 0.05$ vs. the saline-treated control (*t*-test). p-ERK, p-Stat3, and p-Akt: phosphorylated form of ERK, Stat3, and Akt, respectively.

like immunocompetent cells. The present study design cannot distinguish between the direct and indirect effects of the treatments on the heart. Second, G-CSF was originally reported to enhance postinfarct myocardial regeneration by mobilized bone marrow-derived cells to the myocardium (28). This effect is still controversial (11, 18, 21, 28, 32), but we did not examine it in the present study. We also did not address myocardial regeneration from resident cardiac stem cells (20), and the possible effect of G-CSF on such a response remains unresolved.

In conclusion, we found that a combination of G-CSF and sFas gene therapies administered during the subacute stage of MI mitigated cardiac remodeling and dysfunction at the chronic stage more effectively than either of the individual therapies alone. Rapid recanalization of the occluded coronary artery, which enables salvage of ischemic myocardial cells, is presently the best clinical approach to treating acute MI. Unfortunately, most patients lose the chance for coronary reperfusion therapy because reperfusion must be performed within hours after the onset of infarction (30). In that context,

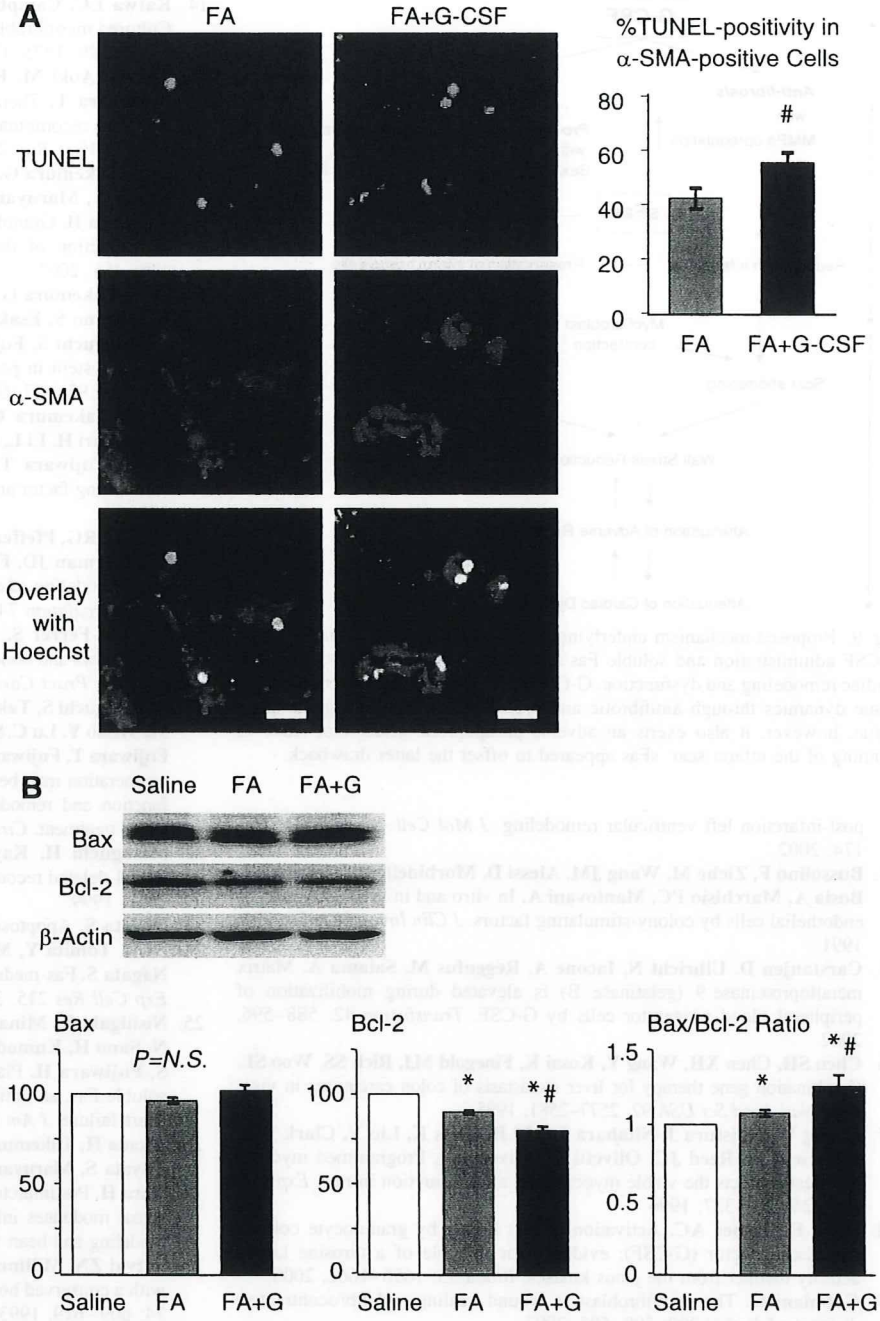

Fig. 8. In vitro effect of G-CSF on Fas-mediated apoptosis among myofibroblasts. *A*: effect of G-CSF on the incidence of Fas-mediated apoptosis among cultured myofibroblasts derived from 1-wk-old infarct tissue. Bars = 20 μm. The graph shows the %TUNEL-positivity among the cells. #$P < 0.05$ vs. FA (agonistic anti-Fas antibody plus actinomycin D)-treated group (*t*-test). *B*: effect of Fas stimulation and the additional treatment with G-CSF on expression of Bax and Bcl-2 in cultured myofibroblasts. *$P < 0.05$ vs. saline-treated control, #$P < 0.05$ vs. FA-treated group (one-way ANOVA).

combination of a cardioprotective cytokine treatment and an antiapoptotic strategy could be a powerful tool for use against the chronic progressive heart failure seen in patients with large MIs, one which could be utilized during the subacute stage, after patients have lost the chance for coronary reperfusion. In contrast to G-CSF, however, safety of systemic delivery of sFas has not been confirmed in humans. Ethical consensus has not been established at all in the safety of a virus-mediated gene therapy. These issues should be resolved before clinical application of the sFas gene therapy.

ACKNOWLEDGMENTS

We thank Kazuko Goto and Hatsue Ohshika for technical assistance.

GRANTS

This study was supported in part by grants-in-aid for scientific research nos. 15209027, 15590732, 14570700, and 13470143 from the Ministry of Education, Science and Culture of Japan.

REFERENCES

1. **Aoyama T, Takemura G, Maruyama R, Kosai K, Takahashi T, Koda M, Hayakawa K, Kawase Y, Minatoguchi S, Fujiwara H.** Molecular mechanisms of non-apoptosis by Fas stimulation alone versus apoptosis with an additional actinomycin D in cultured cardiomyocytes. *Cardiovasc Res* 55: 787–798, 2002.
2. **Avalos BR.** Molecular analysis of the granulocyte colony-stimulating factor receptor. *Blood* 88: 761–777, 1996.
3. **Baldi A, Abbate A, Bussani R, Patti G, Melfi R, Angelini A, Dobrina A, Rossiello R, Silvestri F, Baldi F, Di Sciascio G.** Apoptosis and